THE JOURNAL OF BIOLOGICAL CHEMISTRY VOL. 288, NO. 32, pp. 22993–23008, August 9, 2013


# Dual Roles of the Transcription Factor Grainyhead-like 2 (GRHL2) in Breast Cancer*[S]

Received for publication, January 24, 2013, and in revised form, June 28, 2013 Published, JBC Papers in Press, June 29, 2013, DOI 10.1074/jbc.M113.456293

**Stefan Werner[‡1], Sabrina Frey[‡1], Sabine Riethdorf[‡], Christian Schulze[§], Malik Alawi[¶], Lea Kling[‡], Vida Vafaizadeh[‖], Guido Sauter**, Luigi Terracciano[‡‡], Udo Schumacher[§§], Klaus Pantel[‡], and Volker Assmann[‡2]**

*From the [‡]Department of Tumor Biology, the [§]Center of Molecular Neurobiology Hamburg, the [¶]Bioinformatics Service Facility, and Heinrich-Pette-Institute, Leibniz-Institute for Experimental Virology, Virus Genomics, Hamburg, the **Institute of Pathology and the [§§]Institute of Anatomy II, University Medical Center Hamburg-Eppendorf, D-20246 Hamburg, Germany, the [‖]Institute of Biomedical Research, D-60596 Frankfurt, Germany, and the [‡‡]Institute of Pathology, CH-4003 Basel, Switzerland*

**Background:** The role of the developmental transcription factor GRHL2 in breast carcinogenesis is ill defined.
**Results:** Loss of GRHL2 expression induces an epithelial-to-mesenchymal transition and a reduction in cancer cell proliferation. GRHL2 and ZEB1 transcription factors form a negative feedback loop.
**Conclusion:** GRHL2 exhibits dual roles in breast cancer.
**Significance:** This study suggests the significance of GRHL2 in breast carcinogenesis.

**Using a retrovirus-mediated cDNA expression cloning approach, we identified the grainyhead-like 2 (GRHL2) transcription factor as novel protooncogene. Overexpression of GRHL2 in NIH3T3 cells induced striking morphological changes, an increase in cell proliferation, anchorage-independent growth, and tumor growth *in vivo*. By combining a microarray analysis and a phylogenetic footprinting analysis with various biochemical assays, we identified the epidermal growth factor receptor family member *Erbb3* as a novel GRHL2 target gene. In breast cancer cell lines, shRNA-mediated knockdown of GRHL2 expression or functional inactivation of GRHL2 using dominant negative GRHL2 proteins induces down-regulation of *ERBB3* gene expression, a striking reduction in cell proliferation, and morphological and phenotypical alterations characteristic of an epithelial-to-mesenchymal transition (EMT), thus implying contradictory roles of GRHL2 in breast carcinogenesis. Interestingly, we could further demonstrate that expression of GRHL2 is directly suppressed by the transcription factor zinc finger enhancer-binding protein 1 (ZEB1), which in turn is a direct target for repression by GRHL2, suggesting that the EMT transcription factors GRHL2 and ZEB1 form a double negative regulatory feedback loop in breast cancer cells. Finally, a comprehensive immunohistochemical analysis of GRHL2 expression in primary breast cancers showed loss of GRHL2 expression at the invasive front of primary tumors. A pathophysiological relevance of GRHL2 in breast cancer metastasis is further demonstrated by our finding of a statistically significant association between loss of GRHL2 expression in primary breast cancers and lymph node metastasis. We thus demonstrate a crucial role of GRHL2 in breast carcinogenesis.**

The *Drosophila* gene *grainyhead* (*dGrh*) is the founding member of a large family of genes encoding evolutionarily conserved transcription factors that play key regulatory roles during embryonic development. Based on sequence similarity, members of this gene family are grouped into two different branches (1). One phylogenetic arm, with *Drosophila CP2* (*dCP2*) as an ancestral gene, includes the transcription factors CP2, LBP-1a, and LBP-9. These genes exhibit a wide tissue distribution and regulate diverse cellular processes. The other phylogenetic branch, with *dGrh* as an ancestral gene, encompasses the closely related grainyhead-like (GRHL) transcription factors GRHL1–3 (1–3). In contrast to *dCP2*-related transcription factors, GRHL1–3 proteins exhibit much more restricted and distinct expression patterns during murine development, suggesting that they are not functionally redundant proteins (4). Among the GRHL family members, GRHL2 probably represents the least characterized transcription factor. A fundamental role of GRHL2 proteins in both neural and non-neural developmental processes is reflected by the fact that Grhl2-null mutant mice die by embryonic day 11.5 (5). Grhl2-deficient mice exhibit neural tube closure defects and severe defects in the formation of apical junctional complexes in several types of epithelia (5). A more detailed molecular analysis revealed that GRHL2 regulates epithelial differentiation by directly modulating expression of the adherens junction gene *Cdh1* (E-cadherin) and the tight junction gene *Cldn4* (claudin 4) (5). Likewise, mice with an *N*-ethyl-*N*-nitrosourea-induced nonsense mutation in the *Grhl2* gene die by embryonic day 12.5 due to defects in neural tube closure and heart development (6). Although these and several other developmental studies (4, 7–9) clearly established a crucial role of GRHL2 in embryonic development, an implication of GRHL2 in other physiological processes, such as, for example, wound healing and cancer, is less well defined. This is surprising because two members of the grainyhead family of transcription factors, namely *dGrh* and GRHL3, have attracted considerable interest in that these genes could be identified as important regulators in epithelial barrier formation and wound healing in flies and vertebrates, respec-

* This work was supported by the European Research Council Grant ERC-2010-AdG_20100317 DISSECT (to K. P.).
[S] This article contains supplemental Tables 1 and 2.
[1] Both authors contributed equally to this work.
[2] To whom correspondence should be addressed: Dept. of Tumor Biology, Center of Experimental Medicine, University Medical Center Hamburg-Eppendorf, Martinistrasse 52, 20246 Hamburg, Germany. Tel.: 49-40-7410-56181; Fax: 49-40-7410-56546; E-mail: v.assmann@uke.de.

tively (10–12). It has been known for a long time that wound healing and carcinogenesis represent closely related physiological processes characterized by an increased cell proliferation, extensive tissue remodeling, blood vessel formation, and an inflammatory response (13). Despite fundamental differences between both pathological processes (14), it has been hypothesized that factors involved in wound healing potentially also could play a crucial role in cancer, and vice versa.

To date, however, evidence has been reported for both tumor-promoting and -suppressing activities of the GRHL2 transcription factor in tumorigenesis. For example, GRHL2 has been demonstrated to positively regulate expression of the human telomerase reverse transcriptase (*hTERT*) gene during cellular immortalization of oral squamous cell carcinoma cells (15, 16) and to inhibit apoptosis by suppressing death receptor (FAS and DR5) expression in breast cancer cells (17). GRHL2 also has been shown to regulate proliferation of hepatocellular carcinoma cells (18) while acting as a suppressor of epithelial-to-mesenchymal transition (EMT)[3] in breast cancer (19, 20). Collectively, these observations strongly suggest a fundamental but probably tissue type-specific function of GRHL2 in carcinogenesis.

Using a genetic screen, we identified the GRHL2 transcription factor as a novel protooncogene capable of transforming NIH3T3 fibroblasts. We also provide evidence for dual roles of GRHL2 in breast cancer in that loss of GRHL2 induces a striking reduction in cell proliferation and EMT-like alterations. Moreover, our results further suggest the existence of a highly complex, interconnected GRHL2/ZEB1/miR-200 regulatory network in breast cancer cells. Finally, a comprehensive immunohistochemical analysis of GRHL2 expression in primary breast cancers further demonstrates the pathophysiological relevance of GRHL2 in breast carcinogenesis.

## EXPERIMENTAL PROCEDURES

*Cell Culture, Transfections, and Retroviral Infections*—Murine NIH3T3 fibroblasts, Phoenix ecotropic and amphotropic retroviral packaging cells, and human breast carcinoma cell lines obtained from the Central Cell Service Unit of the Imperial Cancer Research Fund (London, UK) were cultured as described elsewhere (21). For stable transfection of NIH3T3 cells, *GRHL2* cDNAs were RT-PCR-amplified from GI-101 cells with oligonucleotides 5′-TGTCTGCCCATTGCCACGATCCAGG-3′ and 5′-GATTTCCATGAGCGTGACCTTGAAGCC-3′ using *Pfu* DNA polymerase (Stratagene) and were inserted into the bicistronic mammalian expression vector pIRES-N1 containing the CMV promoter/enhancer and *neoR*-selectable marker (22). An expression plasmid encoding an N-terminally truncated (−305 residues) c-RAF kinase (mutant 22W) (23) was generated using standard molecular biology techniques (24). Plasmids were transfected into NIH3T3 cells using Lipofectamine 2000 (Invitrogen), and transfected cell clones were selected with 500 $\mu$g/ml G418. To generate retroviral expression vectors encoding full-length or dominant negative GRHL2 (GRHL2-DN) proteins, cDNAs were RT-PCR-amplified from GI-101 cells using primers 5′-GGATCAAACATGTCACAAGAGTCG-3′ and 5′-TCACGGTGGTGAAAGCTGAAG-3′ (GRHL2-DN) in combination with 5′-GATTTCCATGAGCGTGACCTTGAAGCC-3′, respectively, and were inserted into the pMXs-IP retroviral expression vector. Retroviral infection of target cells was conducted according to standard protocols (24). For induction of EMT, MCF-10A cells were stimulated with 5 ng/ml TGF-$\beta$ (R&D Systems) for 2 days.

*Retrovirus-mediated cDNA Expression Cloning of Protooncogenes*—Poly(A)$^+$ RNA from GI-101 cancer cells prepared with a FastTrack mRNA extraction kit (Invitrogen) was converted into an random-primed, non-directional retroviral cDNA expression library ($>1 \times 10^7$ independent clones, average insert size 1.5 kb) in the retroviral expression plasmid pMXs using the SuperScript plasmid system (Invitrogen). The retroviral cDNA expression library was converted to retroviruses by transient transfection into Phoenix-eco packaging cells. Forty-eight hours post-transfection, the infectious retroviral supernatant was harvested and filtered and was then used to infect NIH3T3 fibroblasts in the presence of 4 $\mu$g/ml Polybrene (Sigma). The medium containing retroviruses was replaced with fresh culture medium 6–8 h after the beginning of the infection, after which the NIH3T3 cell culture was fed at 3-day intervals with fresh medium. Foci, appearing 14 days after reaching cell confluence, were picked from infected NIH3T3 cultures and expanded, and genomic DNA was isolated using a DNeasy tissue kit (Qiagen). Proviral cDNA inserts were recovered with oligonucleotides annealing to retroviral vector sequences (pMXs-1, 5′-GGGTGGACCATCCTCTAGACTGC-3′; pMXs-2, 5′-AACCTACAGGTGGGGTCTTTCATTCC-3′) using *Pfu* DNA polymerase. PCR amplification products were then reintegrated into EcoRI/NotI or BamHI/NotI sites of the pMXs plasmid. Following conversion to retroviruses, individual plasmids were subjected to a second round of selection using the NIH3T3 focus assay. Plasmid clones tested positive for transformation were sequenced, and the identity of cDNA fragments was determined by a BLAST search (25).

*Transformation Assays*—Determination of growth rate, anchorage-independent growth (using soft agar assays), and tumorigenicity in athymic nude (*nu/nu*) mice of parental and transfected NIH3T3 cell clones was performed as described (26).

*Microarray Analysis*—Total RNA was extracted from parental and GRHL2-expressing NIH3T3 cells using the RNeasy kit (Qiagen). For each cell culture, three samples taken from different passages were utilized for expression profiling using Agilent Whole Mouse Genome 4 × 44,000 microarrays (Agilent Technologies) according to the manufacturer's instructions using quantile normalization (27). Differential expression was calculated via fitting expression levels from parental and transfected cell lines to a linear model with moderated *t* statistics. Genes that were at least 2-fold ($\log_2$ scale) up- or down-regulated at an adjusted *p* value of $\leq$1E−5 were considered to be differentially expressed. Microarray data sets are available at the NCBI Gene Expression Omnibus (GEO) Web site under accession code GSE43610.

*Quantitative Real-time RT-PCR Analysis (qRT-PCR)*—Differential mRNA expression was analyzed following extraction

[3] The abbreviations used are: EMT, epithelial-to-mesenchymal transition; MET, mesenchymal-to-epithelial transition; DN, dominant negative; qRT-PCR, quantitative RT-PCR.

of total RNA from cells and reverse transcription using Superscript II (Invitrogen) and random hexamers. First strand reverse transcribed cDNA was then diluted 1:20 in water before use in real-time PCR. Primers were used together with the Quantitect™-SYBR Green-Mastermix (Qiagen) in a Realplex⁴-PCR system (Eppendorf) according to the manufacturer's instructions. Primer sequences and PCR conditions are available upon request. Real-time PCR data analysis was performed using the ΔΔ*CT* method with *RPLP0* or *Gapdh* as an endogenous reference.

*GRHL2 Expression Analysis*—GRHL2 mRNA expression in human breast cancer cell lines was analyzed by Northern blot hybridization of total RNA with a radiolabeled full-length *GRHL2* cDNA essentially as described elsewhere (21). For Western blot analysis of GRHL2 proteins, whole-cell extracts from cultured cells were prepared by lysis of cells directly in SDS sample buffer containing proteinase inhibitors and sonication. Proteins were separated on denaturing 8% polyacrylamide gels and were then subjected to Western blot analysis essentially as described elsewhere (28). To generate polyclonal antibodies against GRHL2, a peptide derived from the central region of human GRHL2 was coupled to keyhole limpet hemocyanin and was then injected into rabbits. GRHL2-specific antibodies were isolated by immunoaffinity purification using the corresponding immunizing peptide coupled to a solid support. Reactivity and specificity of the GRHL2-specific antibodies (anti-GRHL2-P2) was verified by Western blot analysis. Other antibodies used for Western blot analyses include antibodies specific for ERBB3 (clone C17), HSC70 (clone B6), Raf-1 (clone C-12), ZEB1 (clone H-102; all from Santa Cruz Biotechnology, Inc.), Vimentin (clone RV202) and E-cadherin (clone 36) (both from BD Biosciences), N-cadherin (Novus Biologicals), cytokeratin 8 (clone Ks 8.7; Progene), and EPCAM (clone VU-1D9; Novocastra). The anti-CD24 monoclonal antibody (clone SWA11) was kindly provided by P. Altevogt (DKFZ Heidelberg) (29). Analysis of *GRHL2* splice variants by RT-PCR analysis was performed with oligonucleotides 5′-TGTCTGCCCATTGCCACGATCCAGG-3′ and 5′-TACTCTGGGCTTCACTGGTGCCAAGG-3′. Detection of *GRHL2* and β-actin transcripts was performed with the following primers: GRHL2 (5′-AACAGGAAGAAAGGGAAAGGCCAGG-3′ and 5′-TAGATTTCCATGAGCGTGACCTTG-3′) and β-actin (5′-CCTCCCTGGAGAAGAGCTACG-3′ and 5′-AGGACTCCATGCCCAGGAAG-3′).

*Luciferase Reporter Gene Assays*—Promoter elements from the mouse *Erbb3* gene were PCR-amplified and ligated to the *firefly* luciferase reporter gene by insertion into the XhoI/HindIII cloning sites of the pGL4.10 vector (Promega). HEK 293T cells were transiently cotransfected with individual reporter plasmids and either the empty pIRES-N1 vector or the pIRES-N1 vector encoding the FLAG-tagged GRHL2 using Lipofectamine 2000. Cotransfection with the pGL4.74 plasmid containing the *Renilla* luciferase cDNA under the control of the HSV-TK promoter served as a control for the different transfection efficiencies. Forty-eight hours post-transfection, cell extracts were assayed in triplicate for luciferase activities using the Dual-Luciferase reporter assay system (Promega) and a GloMax™20/20 luminometer (Promega). Before calculating the -fold activation value, the luciferase activity of each sample was normalized to the *Renilla* luciferase activity.

*Lentivirus-mediated Knockdown of Gene Expression*—Lentiviral pLKO.1 shRNA vectors targeted against human *GRHL2* (GRHL2#1, TRCN0000015810; GRHL2#2, TRCN0000015812) and human *ZEB1* (ZEB1#1, TRCN0000017563; ZEB1#2, TRCN0000017565) were obtained from the RNAi Consortium (Broad Institute of Harvard and Massachusetts Institute of Technology) (30). pLKO.1 vectors harboring a scrambled nontarget shRNA sequence or a GFP-specific shRNA sequence (Addgene) served as negative controls. Lentiviruses were made by transfection of HEK 293T packaging cells with these constructs by using a three-plasmid system according to standard protocols. Supernatants were harvested, sterile filtered, and then used to infect target cells in the presence of 8 μg/ml Polybrene. Pooled stable transfectants were established using puromycin selection. Stable transfectant cells were maintained in medium containing 1 μg/ml puromycin.

*Electrophoretic Mobility Shift Assay (EMSA)*—Nuclear protein extracts were prepared as described elsewhere (31). Oligonucleotides derived from the regulatory regions of murine *Erbb3* (Erbb3-WT, 5′-AAGTGATCCAACCGGCTAGGGGAGTT-3′) or human *GRHL2* (GRHL2-WT, 5′-AGAAGGGCCTTACCTGAGCGCGCCTC-3′) were end-labeled using [γ-$^{32}$P]ATP and T4 polynucleotide kinase (New England Biolabs), followed by ProbeQuant G-50 microcolumn purification (GE Healthcare). Binding reactions were carried out in a 15-μl volume containing 5 μg of nuclear protein extract, 5 μl of 3× binding buffer (20 mM HEPES/KOH, pH 7.9, 60 mM KCl, 1 mM DTT, 1 mM EDTA, 12% glycerol), 50 ng/μl poly(dI-dC) (Roche Applied Science), and about 50 000 cpm of $^{32}$P-labeled oligonucleotide for 30 min at 4 °C. Competition assays were performed in the presence of a 50-fold molar excess of unlabeled wild-type or mutant oligonucleotides (Erbb3-Mut, 5′-AAGTGATCCAAACGTCTAGGGGAGTT-3′; GRHL2-Mut, 5′-AGAAGGGCCTTACCGGAGCGCGCCTC-3′), respectively. Specificity of binding was further demonstrated by a supershift/competition assay using anti-ZEB1 (clone H-102) and anti-NFκB p65 (clone A) antibodies (all from Santa Cruz Biotechnology, Inc.) for 30 min at 4 °C. Retarded complexes were separated from free probe by electrophoresis on native 4% polyacrylamide gels in 0.5× TBE buffer and were then visualized by autoradiography of the dried gels.

*In Silico Promoter Analyses*—For *in silico* analysis of promoter sequences, we focused on significantly differently expressed genes (adjusted *p* value ≤ 1E−5) for which mouse-human ortholog pairs were available from Ensembl Biomart (release 69) (32). Briefly, promoter sequences (1 kb upstream) for transcripts flagged as belonging to the consensus coding sequence (CCDS) at respective gene loci were obtained. Sequences were analyzed for individual matches of the GRHL2 motif defined by a frequency matrix (9), using a regulatory sequence analysis tool (RSAT, matrix-scan, upper threshold 1E−3, organism-specific background) (33). Reported normalized weights for unique sites were averaged per gene per species and across all hits. Gene ontology terms were also obtained from the Ensembl Biomart service. Putative transcription factor binding sites located within the proximal promoter of *GRHL2* (1 kb upstream of the transcription start site) were

extracted from the UCSC track "Transcription Factor ChIP-seq" from ENCODE (34) using an in-house Ruby script. The ZEB1 ChIP-seq peak (chr8: 102504446–102504669) was then screened for exact matches of putative ZEB1 binding sites (35). The software MUSCLE (version 3.8.31) (36) was employed to calculate a multiple-sequence alignment using the ZEB1 ChIP-seq peak sequence and homologous sequences from chimpanzee, mouse, cattle, and chicken. Sequence alignment was visualized using Unipro UGENE software (37).

*Chromatin Immunoprecipitation (ChIP) Assay*—ChIP assays were performed using a ChIP-IT assay kit (Active Motif) according to the manufacturer's instructions with slight modifications. Briefly, cells were cross-linked with 1% formaldehyde in culture medium for 5 min at room temperature. After cell lysis, chromatin was fragmented by sonication. A fraction of soluble chromatin was saved for measurement of total chromatin input. ChIP assays were performed using antibodies specific for GRHL2 (anti-GRHL2-P2 and anti-GRHL2 (A01); Abnova) or ZEB1 (clone H-102 (Santa Cruz Biotechnology, Inc.) and clone HPA027524 (Sigma)). In control experiments, no antiserum or negative and positive control antibodies provided by the manufacturer (Active Motif) were used. DNA was purified from the immunoprecipitates using a PCR purification kit (Qiagen). Subsequently, promoter sequences were PCR-amplified using primers specific for the *Erbb3* (5′-GAGGTGGCATGAACGCTAG-3′ and 5′-GATGCGCGTAAGTGATGGAAAG-3′) or GRHL2 (5′-CCACAATCCCTAGTGTTTGCAGGTGTTGC-3′ and 5′-CTAAAGGGTACAAGCCCGAGGGACGAGC-3′) regulatory regions, respectively. Murine and human GAPDH promoter-specific primers (Active Motif) were used in negative control reactions. PCR products were separated on 2% agarose gels and were visualized by ethidium bromide staining.

*Immunohistochemistry*—Paraffin-embedded tissue specimens of 55 breast cancer patients and a high density breast cancer prognosis tissue micoarray containing 36 control tissues, 34 normal breast tissues, and 2271 formalin-fixed, paraffin-embedded primary breast tumor specimens with available clinical follow-up and histopathologic data (38) were evaluated immunohistochemically for GRHL2 expression. Tissue sections were deparaffinized and then were subjected to pressure cooker pretreatment in citrate buffer (BioGenex) for 5 min at 125 °C. After blocking of endogenous peroxidase activity using DAKO REAL™ peroxidase blocking solution (Dako), the polyclonal anti-GRHL2-P2 antibody (1:500 dilution) was applied overnight at 4 °C. Subsequently, slides were incubated with peroxidase-labeled EnVision™ polymer coupled with goat anti-rabbit/mouse immunoglobulins (Dako) for 15 min at room temperature. GRHL2 expression was visualized using 3,3′-diaminobenzidine as chromogen in substrate buffer containing hydrogen peroxide. Finally, sections were counterstained with Mayer's hemalaun solution (Merck) and permanently mounted. For negative controls, the addition of primary antibodies was omitted. Staining intensity was estimated on a four-step scale (0, 1, 2, 3). The intensity of the nuclear GRHL2-specific immunoreaction was grouped into low (negative or weak) and high (moderate and strong).

*Statistical Analyses*—Calculations were performed using SPSS for Windows, version 18.0 (SPSS Inc., Chicago, IL). Correlations between GRHL2 expression in breast cancer tissues and clinicopathological parameters were analyzed by $\chi^2$ or Fisher's exact tests. Two-tailed $p$ values below 0.05 were considered statistically significant. Data from functional assays represent an average of at least triplicate samples. *Error bars* represent S.D. All experiments were repeated at least three times. Statistical significance was determined by the Mann-Whitney $U$ test, and $p < 0.05$ was considered significant.

## RESULTS

*Transforming Activities of the GRHL2 Transcription Factor*—To identify genes possibly involved in breast carcinogenesis, a retrovirus-mediated cDNA expression cloning approach for the identification of protooncogenes, utilizing preneoplastic NIH3T3 fibroblasts as a recipient cell line, was employed. Briefly, a retroviral cDNA expression library prepared from GI-101 mammary carcinoma cells was converted to retroviral particles for the infection of contact-inhibited NIH3T3 fibroblasts. Foci appearing 2 weeks after cell confluence were isolated and expanded to isolate genomic DNA. To achieve a plasmid rescue, proviral cDNA inserts, recovered by PCR using primers derived from the retroviral expression plasmid, were reintegrated into the retroviral expression vector. Subsequently, individual expression constructs were subjected to a second round of selection using the NIH3T3 focus assay. Finally, the identities of cDNA clones exhibiting transforming activity were determined by DNA sequencing and BLAST search. Using this approach, a large number of cDNA clones with transforming activity was retrieved. As a proof-of-principle, the list of identified protooncogenes encompassed several well characterized oncogenes (*e.g. RAF1*, *VAV2*, and *ECT2*). Interestingly, two independent cDNA clones (positions 1–2390 and 1–3459 of the *GRHL2* cDNA sequence (GenBank™ accession number NM_024915]) coding for the canonical, full-length GRHL2 isoform were also isolated. Deviations from the published *GRHL2* cDNA could not be identified by DNA sequencing, suggesting that transforming activity is associated with wild-type GRHL2 proteins and is not related to the presence of mutations within the GRHL2 molecule. To investigate the transforming potential of GRHL2, we stably expressed GRHL2 proteins in NIH3T3 cells (Fig. 1*A*) and subjected transfectants to various *in vitro* and *in vivo* transformation assays. Parental NIH3T3 fibroblasts and cells harboring an empty expression vector or NIH3T3 fibroblasts stably expressing an activated c-RAF kinase served as negative or positive controls, respectively. Overexpression of GRHL2 induced striking morphological changes (Fig. 1*B*) and a significant increase in cell proliferation as compared with parental or vector-transfected NIH3T3 cells (Fig. 1*C*). Furthermore, GRHL2 was capable of inducing and sustaining *in vitro* anchorage-independent growth of NIH3T3 cells (Fig. 1*D*). Most importantly, GRHL2 also promoted rapid tumor growth in nude mice (tumor latency of 13–31 days; Table 1). Thus, our results clearly demonstrate that *GRHL2* represents a novel protooncogene.

Bioinformatic analysis suggested the existence of another *GRHL2* gene transcript coding for a yet fully uncharacterized, var-

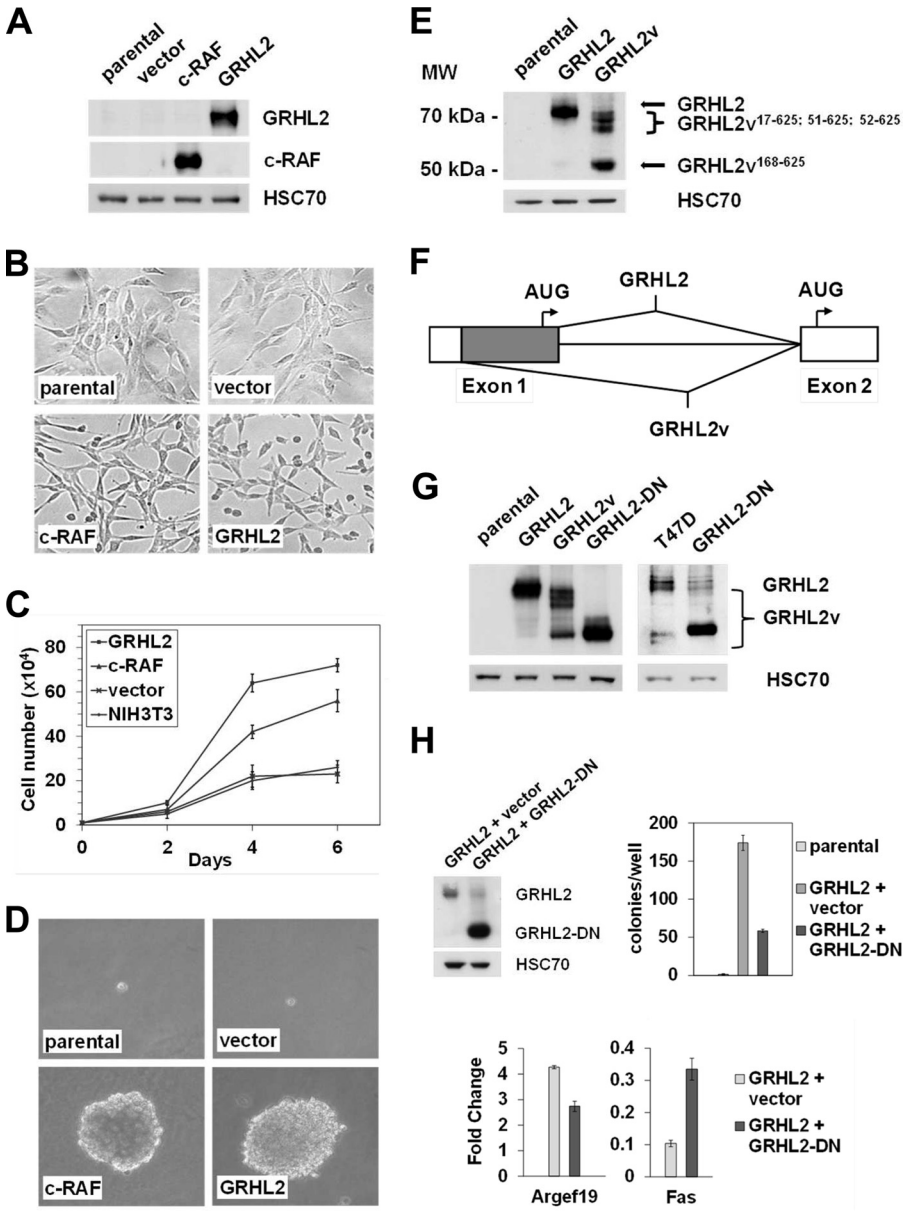


FIGURE 1. **Overexpression of *GRHL2* induces oncogenic transformation of NIH3T3 fibroblasts.** *A*, NIH3T3 fibroblasts were stably transfected with an expression plasmid encoding GRHL2 or activated c-RAF kinase as confirmed by Western blot analysis using antibodies specific for GRHL2 (*top*) or c-RAF kinase (*middle*). Equal loading was demonstrated using an antibody recognizing HSC70 protein (*bottom*). *B*, *GRHL2* mediates a morphological transformation of NIH3T3 fibroblasts. Parental cells, NIH3T3 cells transfected with empty vector, and NIH3T3 cells expressing an activated c-RAF kinase served as negative and positive controls, respectively. *C*, growth characteristics of NIH3T3 cells expressing *GRHL2*. Cells were plated at an initial density of $1 \times 10^4$ cells/well in 6-well plates in growth medium on day 0. Cells from replicate plates were counted at the intervals indicated. *D*, *GRHL2* induces anchorage-independent growth of NIH3T3 fibroblasts. Cells were analyzed for their ability to grow in soft agar. Growth of colonies in semisolid medium was visualized under a light microscope. Representative colony sizes after 14 days are shown. Quantitative data are included in Table 1. *E*, detection of *GRHL2* gene products in NIH3T3 cells stably transfected with expression constructs encoding canonical (GRHL2) or variant GRHL2 proteins (GRHL2v) by Western blot analysis using a GRHL2-specific antibody. *F*, generation of alternate *GRHL2* mRNAs by alternative splicing of the *GRHL2* primary gene transcript (illustration is not to scale). *G*, expression of dominant negative GRHL2 (GRHL2-DN) proteins lacking the first 167 residues (GRHLv(168–625)) in NIH3T3 (*left*) or T47-D cells (*right*). GRHL2 proteins were detected by Western blot analysis using a GRHL2-specific antibody. *H*, functional inactivation of *GRHL2* by GRHL2-DN. *GRHL2*-transfected NIH3T3 cells were retrovirally transduced with an empty vector or an expression plasmid encoding GRHL2-DN proteins as verified by Western blot analysis using a GRHL2-specific antibody (*left*). The dominant negative effect of GRHL2-DN proteins on *GRHL2* activity was confirmed by inhibition of *GRHL2*-induced anchorage-independent growth of NIH3T3 fibroblasts in soft agar (*right*) and by qRT-PCR analysis of GRHL2 target gene expression (*bottom*). -Fold change indicates alterations in expression of positively (*Argef19*) or negatively regulated (*Fas*) *GRHL2*-dependent genes relative to parental cells. *Error bars*, S.D.

iant GRHL2 isoform (GRHL2v). In contrast to canonical GRHL2, GRHL2v exhibited no oncogenic potential in NIH3T3 cells. Remarkably, in GRHL2v-transfected NIH3T3 cells, multiple GRHL2v gene products with apparent molecular masses of 54 kDa (major band) and 65–70 kDa (minor bands) could be detected by Western blot analysis using a GRHL2-specific antibody (Fig. 1*E*). Sequence alignment of both *GRHL2* mRNAs (Ensembl Transcript ID ENST00000251808 and ENST00000395927) showed that an internal 5′ splicing site (AGGT; positions 146–150) within the first exon of the *GRHL2* gene is used to generate an alternate *GRHL2-002* mRNA with a 203-base deletion containing the first AUG codon in its 5′-end. Therefore, initiation of transla-

**TABLE 1**
**Growth properties of GRHL2-transfected NIH3T3 cells**

| Cell line | Morphology[a] | Numbers of colonies in soft agar[b] | Tumorigenicity in nude mice[c] | |
|---|---|---|---|---|
| | | | Tumors/injection | Latency (days) |
| NIH3T3 | Flat | ≤1 | 0/5 | NA[d] |
| NIH3T3/vector | Flat | ≤1 | 0/5 | NA |
| NIH3T3/c-raf (22W) | Spindle-shaped | 221 ± 29 | 5/5 | 13–19 |
| NIH3T3/GRHL2 | Round | 199 ± 21 | 5/5 | 13–31 |

[a] As shown in Fig. 1*A*.
[b] Cells ($3 \times 10^3$) were suspended in a 0.35% agar solution and overlaid onto a 0.5% agar solution in growth medium in 60-mm dishes. One day after incubation, 2 ml of growth medium was added, and colonies were counted 14 days after plating. Each value represents the averages of three experiments with S.D. Representative colony sizes are shown in Fig. 1*C*.
[c] Cells ($1 \times 10^6$) in 0.2 ml of serum-free DMEM were injected subcutaneously into the scapular region of 6–8-week-old female nude mice (5 mice/group). Mice were checked daily for tumor formation at the site of inoculation for up to 70 days. Latency period was the time in days to produce visible tumors.
[d] NA, not applicable.

tion of the *GRHL2-002* transcript predictably occurs at the second AUG within exon 2 and results in an N-terminally truncated (−16 residues) GRHL2v isoform (GRHL2v(17–625)) with a disrupted transactivation domain (Fig. 1*F*). However, a computational analysis of the translation initiation site showed that the first AUG codon of the alternate *GRHL2* mRNA is in a highly unfavorable sequence context for initiating translation (39), suggesting that translation of the *GRHL2-002* mRNA could be initiated from downstream in-frame AUG codons. In fact, the pattern of GRHL2v gene products detected by Western blot analysis corresponded well with the calculated sizes of predicted GRHL2v(17–625), GRHL2v(51–625), GRHL2v(52–625), and GRHL2v(168–625) proteins. To verify our hypothesis, we generated an expression plasmid encoding the putative major GRHL2v gene product (GRHL2v(168–625); hereafter designated as GRHL2-DN) and retrovirally introduced it into NIH3T3 cells. A Western blot analysis showed that GRHL2-DN proteins co-migrate exactly with the major GRHL2v gene product and also with a smaller sized GRHL2 protein detectable in breast cancer cell extracts (Fig. 1*G*; see also Fig. 3), suggesting a physiological relevance of GRHL2-DN proteins. To test whether GRHL2-DN proteins lacking the entire transactivation domain may exhibit dominant negative activity, we retrovirally transduced GRHL2-transformed NIH3T3 cells with a GRHL2-DN expression plasmid (Fig. 1*H*). GRHL2-DN was found to reverse morphological transformation of cells, to drastically reduce the ability of GRHL2-transformed NIH3T3 cells to grow in semisolid medium, and to significantly inhibit GRHL2-mediated gene expression (Fig. 1*H*). Collectively, these results led us to conclude that only the canonical GRHL2 isoform exhibits oncogenic potential, whereas the major GRHL2v gene product (GRHL2-DN) acts in a dominant negative fashion.

*Identification of Erbb3 as a GRHL2 Target Gene*—To better understand GRHL2-dependent regulatory networks leading to oncogenic transformation, it was important to identify potential GRHL2 target genes. To this end, a dual strategy combining gene expression analysis and a phylogenetic footprinting analysis was pursued. A comprehensive overview on *GRHL2*-responsive genes in our cell system was obtained by extracting total RNA from parental and GRHL2-expressing NIH3T3 cells and performing an expression profiling through high density oligonucleotide microarray analysis. A total of 637 genes were identified as being differentially expressed in GRHL2-expressing cells (253 up-regulated and 384 down-regulated), taking a cut-off of an at least 2-fold change in expression relative to parental NIH3T3 fibroblasts at the generally accepted significance threshold (multiple test corrected $p$ value ≤0.05). To identify potential GRHL2 target genes, an *in silico* promoter analysis of regulatory regions of genes differentially expressed between parental and GRHL2-expressing NIH3T3 cells was performed. We also considered the phylogenetic conservation of these binding sites, assuming that motifs with a high degree of interspecies conservation are those that are most likely to have a physiologic relevance. We confined our analysis therefore to genes for which Ensembl lists a 1:1 ortholog mapping ($n$ = 121). The GRHL2 motif was represented by a position frequency matrix constructed from sequences recognized by the GRHL2 transcription factor (9). Using these criteria, we were able to identify 73 genes among our microarray candidate genes predicted to include a putative high scoring GRHL2 recognition sites in their promoter region. The validity of our computational analysis is demonstrated by the fact that the Rho guanine nucleotide exchange factor 19 (*Arhgef19*; mean score 0.97) and the death receptor *Fas* (mean score 0.92), both of which already have been shown to be directly regulated by GRHL2 (17), top the list of highest scoring, putative GRHL2 target genes (supplemental Table 1). Restricting the list of putative GRHL2 target genes to those flagged with the Gene Ontology term "regulation of cell proliferation," *Erbb3*, *Fgfr2*, *Igf2*, *Fas*, and *Stat5a* were considered relevant targets.

To experimentally validate the results obtained by phylogenetic footprinting analysis, we selected the *Erbb3* gene, which is known to play a crucial role in carcinogenesis, for further studies. Computational analysis of the murine *Erbb3* promoter region demonstrated the presence of a single conserved GRHL2 DNA-binding site (AACCGGCT) upstream of the transcription start site (from base pair −371 to −364). Binding of GRHL2 to the predicted DNA-binding site was demonstrated by EMSA (Fig. 2*A*). Additionally, reporter gene assays using various wild-type or mutant murine *Erbb3* promoter fragments linked to the *firefly* luciferase gene showed that activation of the murine *Erbb3* promoter through GRHL2 is strictly dependent on the presence of an intact GRHL2 DNA-binding motif (Fig. 2*B*). Results obtained by phylogenetic footprinting analysis also were confirmed by ChIP assays showing occupancy of the *Erbb3* promoter by GRHL2 proteins *in vivo* (Fig. 2*C*). In summary, our results strongly suggest that *Erbb3* represents a novel GRHL2 target gene.

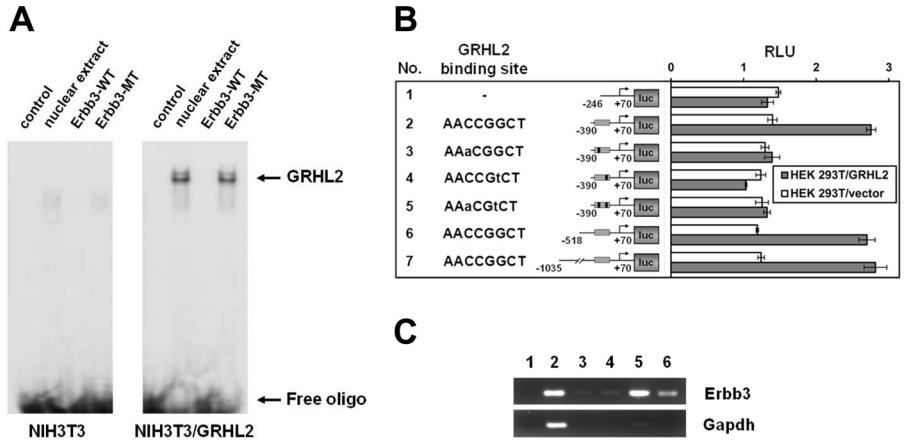


FIGURE 2. **Regulation of *Erbb3* gene expression by GRHL2.** *A*, binding of GRHL2 to a single conserved GRHL2 DNA-binding site within the regulatory region of murine *Erbb3* was demonstrated by EMSA. Nuclear extracts prepared from parental and *GRHL2*-transfected NIH3T3 cells were incubated with a radiolabeled oligonucleotide containing the AACCGGCT sequence, and binding was analyzed by EMSA. Positions of free and bound $^{32}$P-labeled probes are indicated on the *right*. A binding reaction without nuclear extract served as a negative control. The specificity of the shift in migration of the labeled probe was demonstrated by competition EMSA using a 50-fold molar excess of unlabeled consensus (*Erbb3-WT*) or mutant (*Erbb3-MT*) oligonucleotides, respectively. Retarded complexes were separated from free probe by electrophoresis on native 4% polyacrylamide gels and were then visualized by autoradiography of the dried gels. *B*, a panel of reporter constructs was generated in which various wild-type or mutant mouse *Erbb3* promoter fragments were linked to the *firefly* luciferase gene as indicated. The human embryonic kidney cell line HEK 293T was cotransfected with individual reporter constructs and a mammalian expression plasmid encoding the human GRHL2 protein (*shaded bars*). Transfection of an empty expression vector with the reporter construct served as a control (*open bars*). For normalization, a cotransfection with the pGL4.74 plasmid containing the *Renilla* luciferase was performed. Each experiment was performed in triplicate. *Error bars*, S.D. *C*, binding of GRHL2 to the murine *Erbb3* promoter *in vivo* as demonstrated by ChIP assay. Cross-linked protein/chromatin complexes were enriched from *GRHL2*-transfected NIH3T3 cells with two different GRHL2-specific antibodies, anti-GRHL2-P2 (*lane 5*) and anti-GRHL2 (A01) (*lane 6*). Omitting sera (*lane 3*) or using negative control mouse IgG (*lane 4*) served as controls in these experiments. Input chromatin for each experiment is shown in *lane 2*. The immunoprecipitated chromatin was subjected to PCR amplification using primers flanking the *GRHL2*-binding site in the *Erbb3* regulatory region (*top*) or primers specific for the *Gapdh* promoter, which were used as a negative control (*bottom*). In control PCRs, input chromatin was omitted (*lane 1*).

*Growth-promoting Activities of GRHL2 in Human Breast Cancer Cells*—To investigate whether GRHL2 also exhibits growth-promoting activities in human breast cancer cells, we first analyzed the expression of GRHL2 gene transcripts and proteins in a panel of human breast cancer cell lines. GRHL2 expression could be detected in eight of ten breast cancer cell lines at highly variable levels, as determined by Western blot analysis using an in-house GRHL2-specific polyclonal antibody and Northern blot hybridization, respectively (Fig. 3, *A* and *B*). The level of GRHL2 protein expression in each individual cell line corresponded well with the level of *GRHL2* mRNA detected in these cells. Interestingly, GRHL2 isoform expression could be detected in all GRHL2-positive breast cancer cell lines by Western blot analysis (Fig. 3*A*) and non-quantitative RT-PCR analysis (Fig. 3*C*). It is important to note that the poorly differentiated, highly metastatic breast cancer cell lines MDA-MB-231 and BT-549 belonging to the "basal-B" subclass of breast cancer cell lines (40) were completely negative for GRHL2.

To examine whether GRHL2 promotes tumor growth, we first performed a series of lentivirus-mediated RNAi experiments to suppress GRHL2 expression in a variety of GRHL2-expressing breast cancer cell lines (*e.g.* MCF-7, ZR-75-1, T47-D, and MDA-MB-468 cells). Two hairpin shRNAs that efficiently knocked down GRHL2 expression in breast cancer cells as compared with control cells (up to 90% silencing, as confirmed by Western blot analysis; Fig. 4*A*) could be identified. Interestingly, shRNA-mediated knockdown of GRHL2 expression in breast cancer cell lines caused cells to adopt a flat and significantly enlarged morphology. GRHL2-depleted breast cancer cells formed less prominent cell-cell contacts and exhibited increased cell scattering. In addition to these EMT-

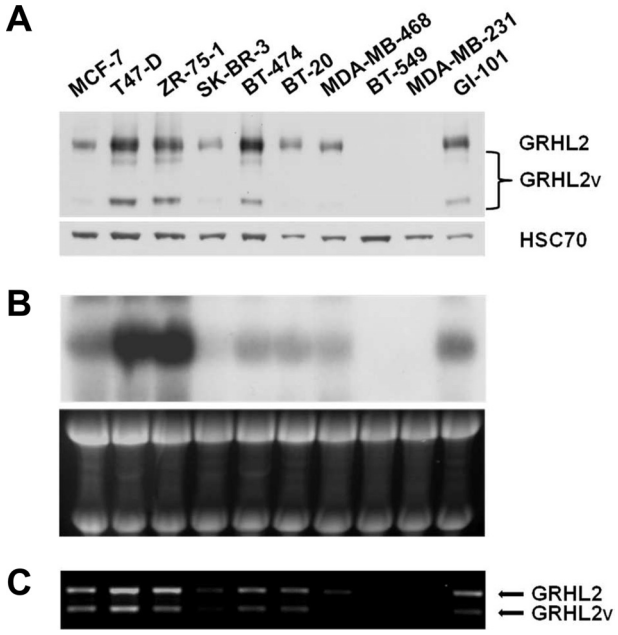


FIGURE 3. **Differential expression of GRHL2 in human breast cancer cell lines.** *A*, expression of canonical (GRHL2) and variant GRHL2 (GRHL2v) proteins in a panel of human breast carcinoma cell lines was determined by Western blot analysis using the in-house GRHL2-specific polyclonal antibody GRHL2-P2. It is noteworthy that variant GRHL2 proteins can be readily detected in all *GRHL2*-positive breast cancer cell lines upon overexposition of the autoradiograph. Equal loading was demonstrated using an antibody recognizing HSC70 protein. *B*, *GRHL2*-specific gene transcripts were detected by Northern blot analysis of total RNA extracted from breast cancer cell lines using a radiolabeled *GRHL2* cDNA. Staining of the gel with ethidium bromide served as a loading control in this experiment. *C*, detection of *GRHL2* splice variants in breast cancer cell lines by non-quantitative RT-PCR analysis. PCR amplification products were visualized by ethidium bromide staining of the agarose gel. PCR products representing the canonical (GRHL2) and variant *GRHL2* gene transcripts (GRHL2v) are indicated by *arrows*, respectively.

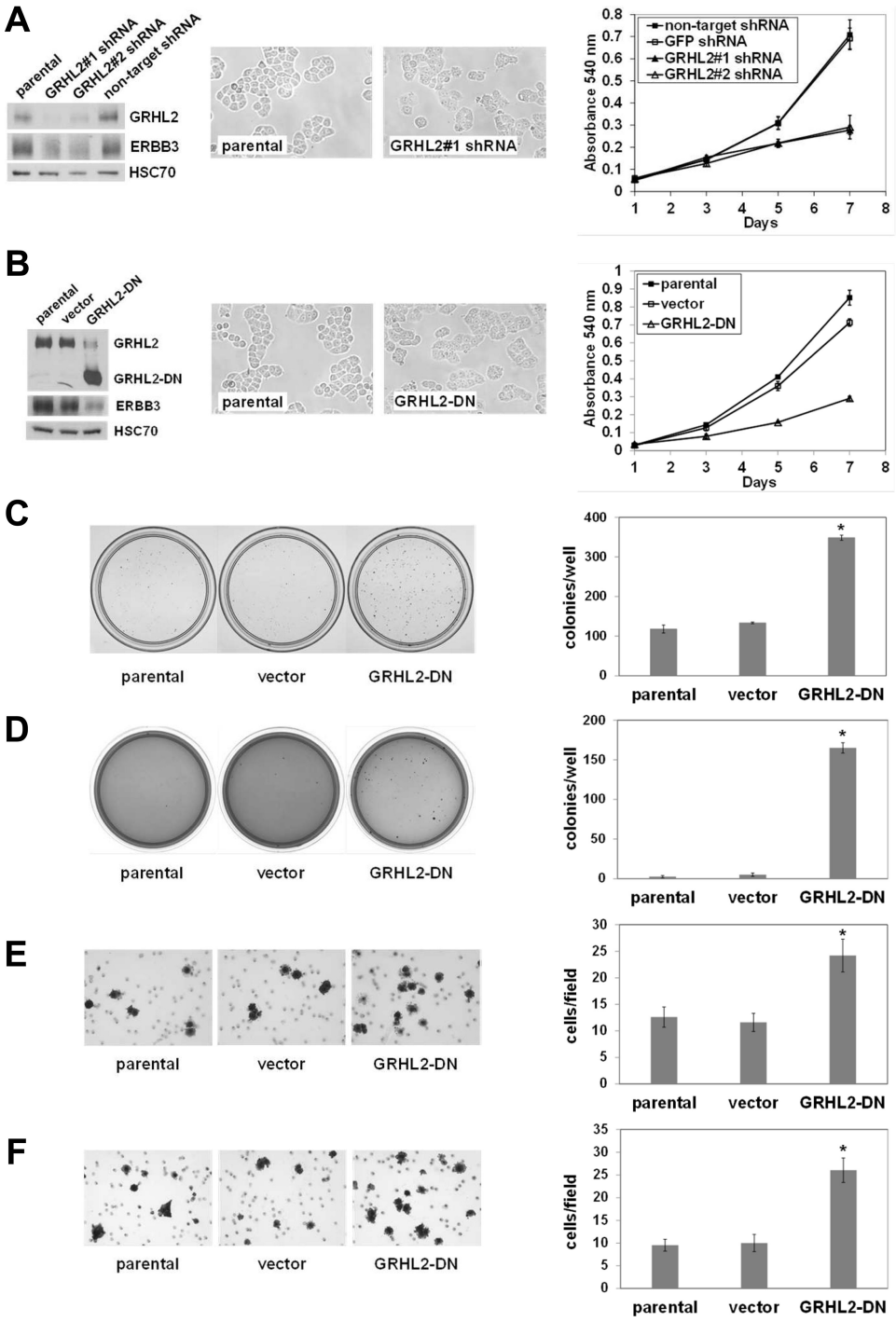


FIGURE 4. **Loss of GRHL2 induces EMT-like phenotypical alterations and a reduction in breast cancer cell proliferation.** *A*, an shRNA-mediated knockdown of *GRHL2* expression in MDA-MB-468 breast cancer cells was achieved by two different shRNAs (GRHL2#1 shRNA and GRHL2#2 shRNA) as determined by Western blot analysis (*left*). Suppression of *GRHL2* expression caused morphological alterations characteristic of an EMT (*middle*) and also a striking reduction in cell growth (*right*). *B*, functional inactivation of *GRHL2* by retroviral transduction of MDA-MB-468 cells with an expression construct encoding dominant negative GRHL2 (GRHL2-DN) proteins (*left*) resulted in EMT-like morphological changes (*middle*) and a remarkable reduction in cell proliferation (*right*). shRNA-mediated knockdown of *GRHL2* expression and functional inactivation of *GRHL2* by means of dominant negative GRHL2 proteins uniformly resulted in a repression of ERBB3 expression in MDA-MB-468 cells as determined by Western blot analysis using an ERBB3-specific antibody (*A* and *B*, *left*). *C*, the ability of single MDA-MB-468 breast cancer cells to form colonies was analyzed in a clonogenic assay. Retrovirally transduced MDA-MB-468 cells expressing GRHL2-DN proteins were plated at an initial density of $1 \times 10^3$ cells/60-mm plate. Colonies appearing 10 days after plating were stained with 0.005% crystal violet in 20% methanol and quantified. *D*, anchorage-independent growth of MDA-MB-468 breast cancer cells was assessed by a soft agar assay. For each cell line, $1 \times 10^4$ cells were mixed with 0.33% agar in growth medium and overlaid on 0.5% agar in a 60-mm plate. After 4 weeks of incubation, colonies were stained with 0.005% crystal violet and counted. *E*, migration of MDA-MB-468 cells was analyzed in a Boyden chamber assay using complete medium as a chemoattractant for 20 h. Cells were fixed with 4% paraformaldehyde and stained with a saturated crystal violet solution. Five randomly chosen fields per membrane were counted at a magnification of ×200. *F*, invasion of MDA-MB-468 cells was analyzed in a Boyden chamber coated with Matrigel using complete medium as chemoattractant for 20 h. Cells were fixed, stained, and quantified as described above. Columns are the mean of a representative experiment assayed in triplicate. *Error bars*, S.D. *, $p < 0.001$ (Mann-Whitney *U* test).

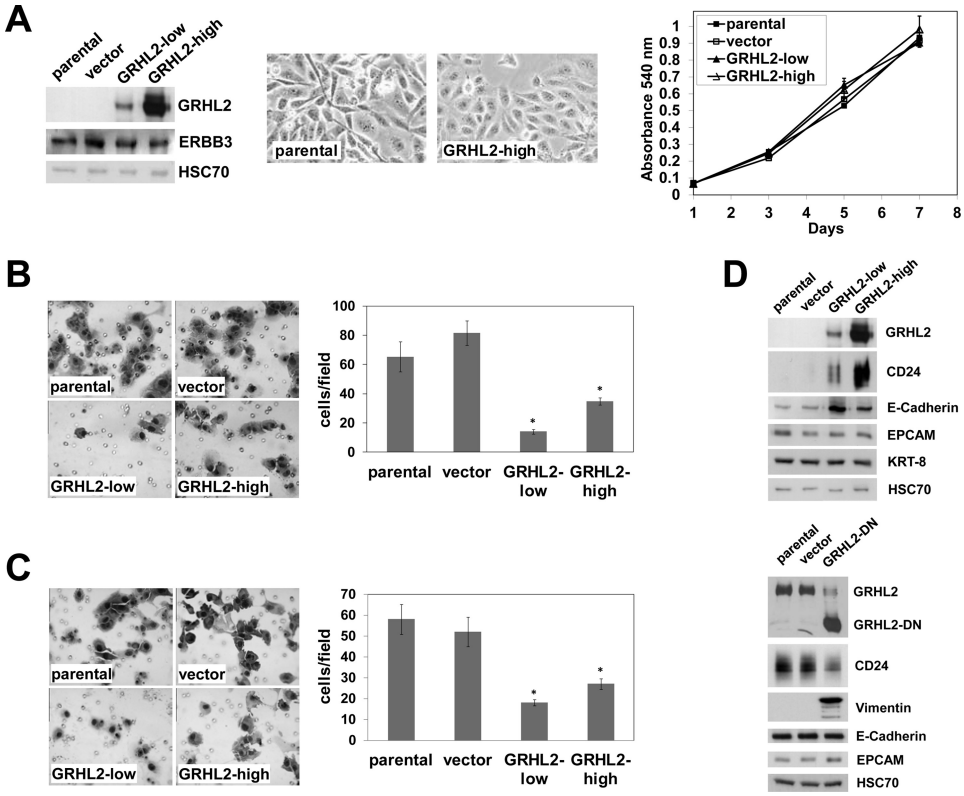


FIGURE 5. **Overexpression of GRHL2 in MDA-MB-231 cells caused MET-like phenotypical changes.** *A*, MDA-MB-231 cells were genetically engineered to stably overexpress *GRHL2* at low and high expression levels as determined by Western blot analysis using a GRHL2-specific antibody. No change in *ERBB3* gene expression was observed (*left*). Forced expression of *GRHL2* in MDA-MB-231 cells induced MET-like morphological changes (*middle*) but did not affect breast cancer cell proliferation as determined by a 3-(4,5-dimethylthiazol-2-yl)-2,5-diphenyltetrazolium bromide assay (*right*). Migration (*B*) and invasion (*C*) of cells was determined in a Boyden chamber assay as described in the legend to Fig. 4. *Columns*, mean of a representative experiment assayed in triplicate. *Error bars*, S.D. *, $p < 0.001$ (Mann-Whitney *U* test). *D*, *GRHL2*-induced changes in expression of selected genes in *GRHL2*-transfected MDA-MB-231 cells (*top*) or MDA-MB-468 cells expressing dominant negative GRHL2 (GRHL2-DN) proteins (*bottom*), as listed in Table 2, were confirmed by Western blot analysis using antibodies as indicated on the *right*. Equal loading was demonstrated using an antibody recognizing HSC70 protein (*A* and *D*).

like morphological changes, a marked down-regulation of ERBB3 protein expression and also a striking reduction in cell growth was observed. Representative results obtained for MDA-MB-468 breast cancer cells are shown in Fig. 4*A*. To further verify these results, we also retrovirally transduced a panel of human breast cancer cell lines with an expression construct coding for dominant negative GRHL2 proteins. We noticed that expression of GRHL2-DN proteins in breast cancer cells provoked a significant suppression of endogenous GRHL2 protein expression (Fig. 4*B*). Functional inactivation of GRHL2 using a dominant negative approach also resulted in EMT-like morphological changes, suppression of *ERBB3* expression, and a remarkable reduction in cell proliferation (Fig. 4*B*). Next, MDA-MB-468 breast cancer cells expressing GRHL2-DN proteins were subjected to various *in vitro* assays. Functional inactivation of GRHL2 using a dominant negative approach significantly increased the ability of individual MDA-MB-468 cells to form colonies in a clonogenic assay (Fig. 4*C*) and to exhibit anchorage-independent growth in soft agar assays (Fig. 4*D*). Moreover, loss of GRHL2 expression also promotes breast cancer cell migration (Fig. 4*E*) and invasion (Fig. 4*F*) in Boyden chamber assays.

We also stably expressed GRHL2 in GRHL2-deficient MDA-MB-231 and BT-549 cells and analyzed its influence on cell proliferation using an 3-(4,5-dimethylthiazol-2-yl)-2,5-diphenyltetrazolium bromide assay. Although forced overexpression of GRHL2 induced morphological changes reminiscent of a mesenchymal-to-epithelial transition (MET), no influence on cell proliferation of either basal-B type of breast cancer cell line could be detected (Fig. 5*A*). *ERBB3* gene expression was found to be unchanged in MDA-MB-231 cells (Fig. 5*A*) or dramatically increased (about 35-fold) in BT-549 cells (data not shown). Overexpression of GRHL2 in MDA-MB-231 cells significantly suppressed cell migration (Fig. 5*B*) and invasion (Fig. 5*C*) in Boyden chamber assays, thus further supporting an EMT suppressor function of GRHL2 in breast cancer cells.

Additionally, we analyzed alterations in expression of EMT-associated genes and selected GRHL2 target genes (*e.g. CDH1* (E-cadherin) and *FAS*) in all three experimental systems by qRT-PCR analysis. Data presented in Table 2 clearly indicate significant changes in a variety of EMT-related genes, including *CDH1* (E-cadherin), *KRT* genes (cytokeratins), *VIM* (vimentin), *CLDN* genes, *DSC2*, *ZEB1*, and *CD24* stem cell marker. GRHL2-induced changes in expression of selected genes were also confirmed by Western blot analysis (Fig. 5*D*). It is interesting to note that alterations in expression of selected GRHL2 target genes were not dose-dependent. For example, induction of E-cadherin and P-cadherin expression is significantly more pronounced in MDA-MB-231 cells expressing relatively low levels of GRHL2 (GRHL2-low) than in the GRHL2-high expres-

**TABLE 2**

**GRHL2-induced alterations in gene expression in experimental breast cancer systems**

Gene expression changes of at least 1.5-fold (up- or down-regulated) relative to controls are considered as significant and are highlighted in boldface type.

| | -Fold change[a] | | | |
|---|---|---|---|---|
| Gene symbol | MDA-MB-231 GRHL2-low | MDA-MB-231 GRHL2-high | MDA-MB-468 GRHL2#1 shRNA | MDA-MB-468 GRHL2-DN |
| DSC2 | **4.19 ± 0.46** | **5.43 ± 0.40** | 1.38 ± 0.16 | −1.47 ± 0.19 |
| DSG2 | 1.37 ± 0.40 | 1.48 ± 0.07 | 1.26 ± 0.26 | −1.49 ± 0.22 |
| DSP | 1.39 ± 0.36 | **2.45 ± 0.95** | 1.36 ± 0.06 | −1.16 ± 0.06 |
| CLDN3 | 1.29 ± 0.20 | **1.58 ± 0.21** | −1.44 ± 0.03 | 1.07 ± 0.27 |
| CLDN4 | **1.70 ± 0.22** | **1.63 ± 0.47** | 1.13 ± 0.05 | 1.08 ± 0.23 |
| CLDN6 | 1.23 ± 0.07 | 1.05 ± 0.29 | 1.07 ± 0.22 | −1.18 ± 0.01 |
| CLDN7 | −1.35 ± 0.11 | −1.08 ± 0.03 | −1.23 ± 0.03 | 1.00 ± 0.18 |
| EPCAM | −1.02 ± 0.06 | 1.22 ± 0.12 | 1.22 ± 0.49 | −1.33 ± 0.01 |
| E-Cadherin | **7.11 ± 0.06** | **2.77 ± 0.33** | −1.28 ± 0.45 | −1.19 ± 0.12 |
| P-Cadherin | **2.11 ± 0.47** | 1.45 ± 0.11 | 1.19 ± 0.06 | 1.14 ± 0.26 |
| OCLN | **2.57 ± 0.76** | **2.89 ± 0.15** | 1.15 ± 0.01 | 1.41 ± 0.27 |
| SMA | 1.15 ± 0.08 | 1.36 ± 0.08 | **2.36 ± 0.01** | **3.05 ± 0.16** |
| ZO-1 | 1.29 ± 0.42 | **2.37 ± 0.73** | 1.02 ± 0.03 | 1.05 ± 0.20 |
| KRT-7 | **1.51 ± 0.03** | **2.71 ± 0.25** | **−1.54 ± 0.12** | **−1.52 ± 0.12** |
| KRT-8 | −1.06 ± 0.19 | 1.14 ± 0.01 | **−1.56 ± 0.02** | **−1.59 ± 0.03** |
| KRT-18 | 1.12 ± 0.17 | 1.32 ± 0.07 | **−1.72 ± 0.32** | **−2.04 ± 0.05** |
| Vimentin | 1.28 ± 0.18 | 1.21 ± 0.35 | **32.65 ± 3.61** | **32.27 ± 3.26** |
| ZEB1 | 1.14 ± 0.30 | 1.27 ± 0.15 | **5.55 ± 0.43** | **5.59 ± 0.53** |
| CD24 | 3.60 ± 0.78 | 6.48 ± 1.64 | **−2.17 ± 0.14** | **−2.27 ± 0.08** |
| CD44 | 1.02 ± 0.04 | 1.13 ± 0.24 | **1.14 ± 0.03** | **−1.45 ± 0.26** |
| ERBB3 | 1.26 ± 0.08 | 1.08 ± 0.04 | **−2.94 ± 0.01** | **−2.27 ± 0.14** |
| FAS | **1.90 ± 0.07** | **5.06 ± 0.50** | 1.22 ± 0.54 | 1.08 ± 0.05 |
| DR4 | **1.80 ± 0.29** | **3.78 ± 0.06** | 1.46 ± 0.14 | 1.11 ± 0.12 |
| DR5 | −1.09 ± 0.03 | −1.10 ± 0.01 | 1.14 ± 0.15 | −1.04 ± 0.39 |
| RAB25 | **11.73 ± 3.60** | **18.54 ± 1.42** | 1.01 ± 0.11 | 1.25 ± 0.04 |
| TERT | **1.69 ± 0.44** | **3.01 ± 0.01** | 1.11 ± 0.00 | 1.16 ± 0.11 |

[a] - Fold change represents alterations in gene expression relative to parental cells as determined by qRT-PCR analysis.

sors. Most importantly, we also found evidence that GRHL2, which was identified as a repressor of death receptor (*FAS*, *DR4*) expression (17), caused a striking up-regulation of *FAS* and *DR4* gene expression in GRHL2-transfected MDA-MB-231 breast cancer cells (Table 2). Collectively, our data strongly suggest that GRHL2 exhibits EMT suppressor activity and regulates *ERBB3* gene expression and cell proliferation of breast cancer cells.

*GRHL2 Antagonizes TGF-β-induced EMT in MCF-10A Cells*—The non-tumorigenic epithelial cell line MCF-10A probably represents the best characterized experimental system for the analysis of TGF-β-induced EMT in human breast cancer (41). To obtain further evidence for a role of GRHL2 in suppressing EMT, we examined GRHL2 mRNA and protein expression in this experimental system. Although *GRHL2* gene transcripts could be detected in MCF-10A cells by non-quantitative RT-PCR analysis at high cycle numbers ($n = 35$), no GRHL2 protein expression could be detected by Western blot analysis using a GRHL2-specific antibody, suggesting a low level expression of *GRHL2* in MCF-10A cells (Fig. 6, *A* and *B*). These observations prompted us to stably express GRHL2 in MCF-10A cells by means of retroviral gene transfer as demonstrated by Western blot analysis (Fig. 6*A*). Although no gross changes in the morphology of infected cells could be observed, we noticed slight morphological changes in subconfluent cultures in that GRHL2-transfected cells showed an increased tendency to grow as even more tightly packed clusters of cells. A qRT-PCR analysis of EMT marker gene expression revealed a striking down-regulation of selected mesenchymal marker proteins (*e.g.* vimentin) and a concomitant up-regulation of epithelial markers (*e.g. CLDN4*), indicating a reinforcement of the epithelial phenotype of MCF-10A cells by GRHL2 (Fig. 6*D*). We next analyzed the effect of TGF-β on parental, empty vector-transfected, and GRHL2-expressing MCF-10A cells and observed striking morphological changes indicative of a fully fledged EMT in parental and vector-transfected but not in GRHL2-expressing MCF-10A cells (Fig. 6*C*). These cells showed only very weak EMT-like morphological changes, and the scattering of cells could hardly be observed. A qRT-PCR analysis of EMT marker gene expression demonstrated a significant suppressive effect of GRHL2 on TGF-β-induced gene expression changes in MCF-10A cells as compared with vector-transfected cells (Fig. 6*D*). GRHL2-induced changes in expression of selected genes were also confirmed by Western blot analysis (Fig. 6*A*). It is important to note, however, that the antagonizing effect of GRHL2 on TGF-β-induced EMT in the MCF-10A experimental system was detectable but less evident when cells were grown in medium containing higher concentrations of TGF-β (10 ng/ml) for extended periods of time (>4 days). Still, our observations further substantiate an EMT suppressor function of GRHL2 in breast cancer cells.

*GRHL2 and ZEB1 Transcription Factors Form a Double Negative Regulatory Feedback Loop*—Little is known about the regulation of GRHL2 gene expression in cancer cells. This prompted us to screen the *GRHL2* regulatory region (1 kb upstream of the transcription start site) for transcription factor binding sites, especially for those known to mediate recruitment of EMT transcription factors. Using *in silico* promoter analysis, we identified three potential binding sites for the ZEB1 transcription factor, which itself very recently has been shown to be regulated by GRHL2 (19), in the human *GRHL2* promoter sequence. ZEB1 has been demonstrated to interact with either E-box elements (especially 5′-CAGGTG-3′, 5′-CATGTG-3′, or 5′-CACCTG-3′) or Z-box elements (especially 5′-CAGGTA-3′ or 5′-TACCTG-3′) in the proximal promoters of target genes, such as, for example, the *CDH1* (E-cadherin) gene (35). A cluster of putative ZEB1 binding sites consisting of two Z-box elements (at positions −129 and −106) and one E-box element (at position −76) was detected (Fig. 7*A*). All three repressive elements evolutionarily were highly conserved, suggesting a physiological relevance.

In fact, analysis of GRHL2 and ZEB1 protein expression in our panel of human breast cancer cell lines by Western blot analysis revealed an inverse pattern of expression (*i.e.* cell lines positive for GRHL2 were negative for ZEB1, and vice versa) (Fig. 7*B*). Next, we performed lentivirus-mediated RNAi experiments to knock down *ZEB1* gene expression in MDA-MB-231 breast cancer cells. Results shown in Fig. 7*C* clearly demonstrate that repression of *ZEB1* expression induces a striking up-regulation of *GRHL2* mRNA and protein expression in MDA-MB-231 cells. To demonstrate involvement of the E/Z-box elements in the recruitment of ZEB1 to the *GRHL2* regulatory region, we also conducted EMSAs using radiolabeled oligonucleotides harboring Z-box 1 and 2- or E-box 1-specific sequences, respectively. Our results clearly indicate significant binding of ZEB1 proteins to all three repressive E/Z-box ele-

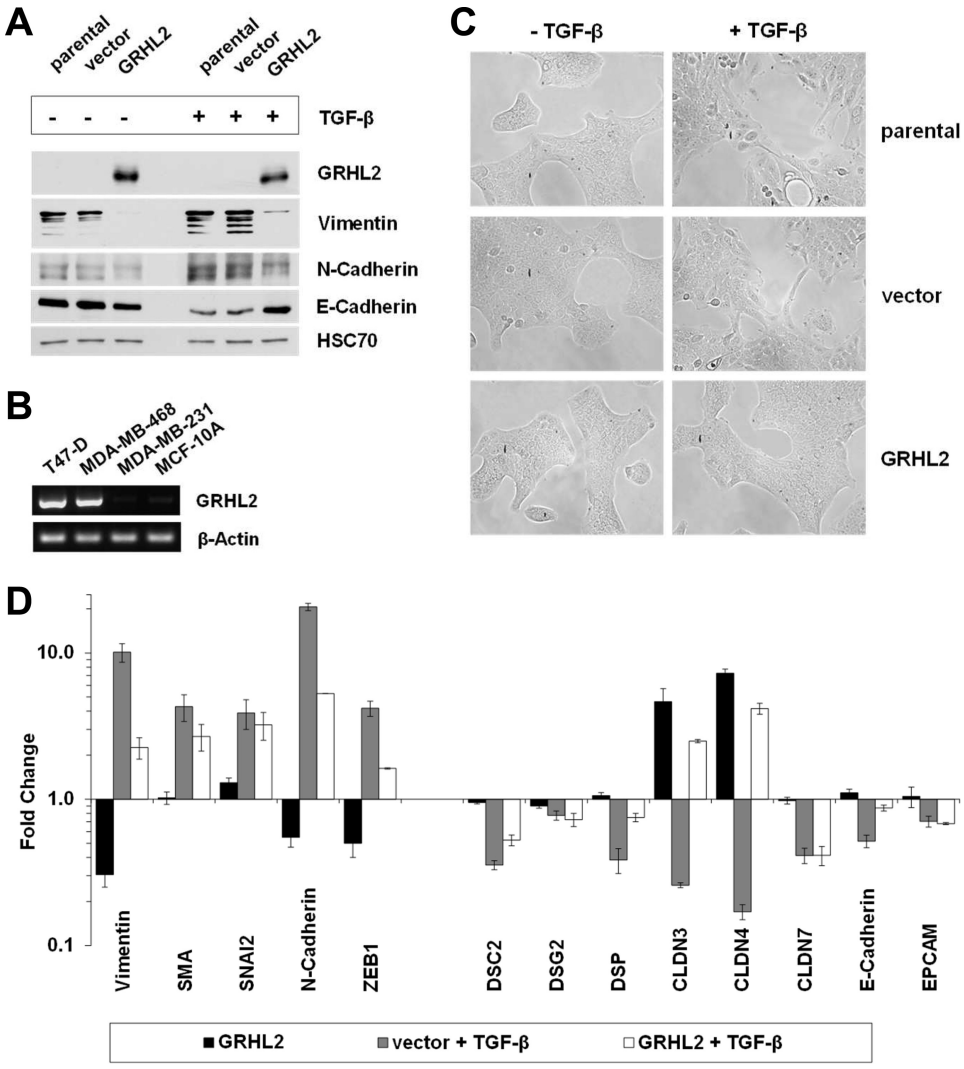


FIGURE 6. **GRHL2 antagonizes TGF-$\beta$ induced EMT in MCF-10A cells.** *A*, GRHL2-deficient MCF-10A cells were genetically engineered to stably overexpress *GRHL2* as confirmed by Western blot analysis using a GRHL2-specific antibody. Changes in expression of selected EMT marker genes in untreated and TGF-$\beta$-stimulated parental, mock-infected, and GRHL2-expressing MCF-10A cells were analyzed by Western blot analysis using the antibodies indicated on the *right*. Equal loading was demonstrated using an antibody recognizing HSC70 protein. *B*, detection of *GRHL2* gene transcripts in selected breast cancer cell lines by non-quantitative RT-PCR analysis. PCR amplification products were visualized by ethidium bromide staining of the agarose gel. T47-D and MDA-MB-468 cells or MDA-MB-231 breast cancer cells served as positive or negative controls, respectively. RT-PCR amplification of *β-actin* mRNA demonstrated the integrity of total RNA used in this experiment. *C*, phase-contrast images of untreated (*left*) or TGF-$\beta$-treated (*right*) parental, vector-transfected, and *GRHL2*-expressing MCF-10A cells. *D*, TGF-$\beta$-induced EMT marker gene expression changes in vector-transfected or GRHL2-expressing MCF-10A cells as determined by qRT-PCR analysis. -Fold change indicates alterations in EMT marker gene expression relative to untreated vector-transfected cells. *Error bars*, S.D.

ments of the *GRHL2* promoter region. Representative results obtained for Z-box 2-derived oligonucleotides and nuclear extracts from MDA-MB-231 cells are shown in Fig. 7*D*. Finally, occupancy of the *GRHL2* promoter by ZEB1 proteins *in vivo* was confirmed by ChIP assays using two ZEB1-specific antibodies (Fig. 7*E*), suggesting that *GRHL2* expression is repressed by the EMT transcription factor ZEB1. Because *ZEB1* previously has been shown to be transcriptionally repressed by *GRHL2* (19, 20) (see also Table 2), our results suggest the existence of a double-negative *ZEB1*/*GRHL2* transcriptional feedback loop in human breast cancer cells.

*Expression of GRHL2 in Human Primary Breast Carcinomas*—To investigate a pathophysiological relevance of a dysregulation of *GRHL2* gene expression in breast cancer, we also evaluated GRHL2 expression in normal and malignant breast tissues by immunohistochemical analysis of a panel of formalin-fixed, paraffin-embedded tissue sections using an in-house GRHL2-specific polyclonal antibody. Representative staining results obtained from a small cohort of tissue specimens ($n = 55$) are shown in Fig. 8. Consistent with its proposed role in epithelial morphogenesis, nuclear GRHL2 expression could be detected in cells of normal mammary glands and in the majority of tumor cells in breast cancer tissues. Interestingly, we also identified a small proportion of primary breast carcinomas without or with only weak GRHL2 expression, suggesting a down-regulation of *GRHL2* expression in these tumors during carcinogenesis. Moreover, we observed a striking loss of *GRHL2* expression in tumor cells at the invasive front and in individual tumor cells with no discernible continuity with the parent tumor (Fig. 8, *B* and *D*). To correlate GRHL2 results obtained by immunhistochemical analysis with clinico-pathological parameters, including age, nodal status, tumor stage, grade of differentiation,

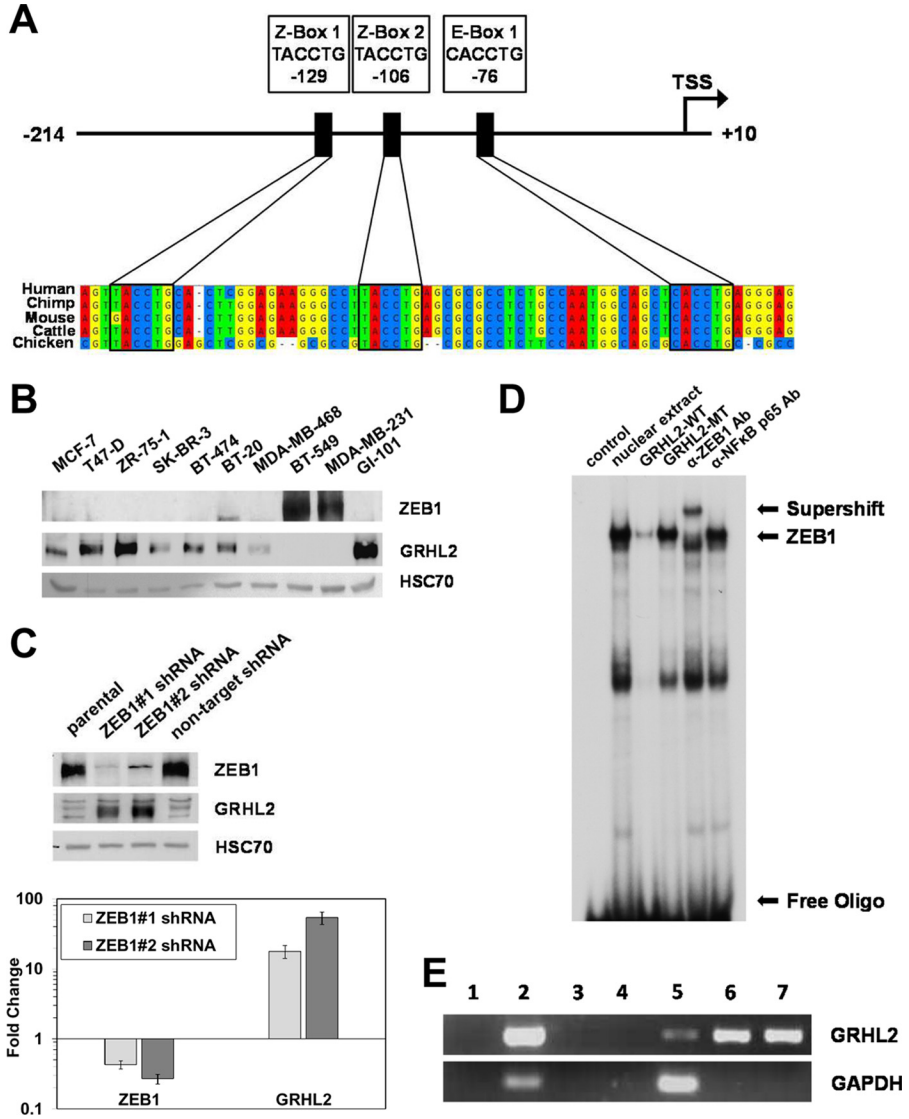


FIGURE 7. **Direct suppression of GRHL2 expression by the transcription factor ZEB1.** *A*, schematic representation of the human *GRHL2* promoter region from positions −214 to +10 relative to the transcription start site (*TSS*) corresponding to the ZEB1 ChIP-seq peak (chr8: 102504446–102504669) as extracted from ENCODE. The relative positions and sequences of E/Z-boxes representing putative binding sites for the transcription factor ZEB1 are indicated. Sequence alignment of *GRHL2* regulatory sequences with the corresponding sequences from chimpanzee, mouse, cattle, and chicken showed a high degree of evolutionary conservation of putative ZEB1 binding sites. *B*, inverse expression pattern of *ZEB1* and *GRHL2* in human breast carcinoma cell lines, as demonstrated by Western blot analysis using antibodies specific for ZEB1 and GRHL2, respectively. Equal loading was demonstrated using an antibody recognizing HSC70 protein. *C*, repression of *ZEB1* expression induces up-regulation of *GRHL2* expression. A stable knockdown of *ZEB1* expression in MDA-MB-231 cells was achieved by lentiviral transduction of cells with two different ZEB1-specific shRNAs (ZEB1#1 and ZEB1#2). Non-infected, parental cells and cells lentivirally transduced with a non-target shRNA served as a control in these experiments. ZEB1 and GRHL2 protein expression levels were assessed by Western blot analysis using antibodies specific for ZEB1 and GRHL2. Equal loading was demonstrated using an antibody recognizing HSC70 protein (*top*). Levels of *ZEB1* and *GRHL2* mRNA expression in pooled stable MDA-MB-231 breast cancer cell lines were determined by qRT-PCR analysis (*bottom*). *D*, binding of ZEB1 to E/Z-box elements within the regulatory region of human *GRHL2* was demonstrated by EMSA. Nuclear extracts prepared from MDA-MB-231 cells were incubated with a radiolabeled Z-box 2-derived oligonucleotide, and binding was analyzed by EMSA. Positions of free probe and shifted and supershifted ZEB1-containing complexes are indicated on the *right*. A binding reaction without nuclear extract served as a negative control. The specificity of the shift in migration of the labeled probe was demonstrated by competition EMSA using a 50-fold molar excess of unlabeled consensus (*GRHL2-WT*) or mutant (*GRHL2-MT*) oligonucleotides, respectively. The specificity of binding was further demonstrated by a supershift assay using anti-ZEB1 or unrelated anti-NFκB p65 antibodies. Retarded complexes were separated from free probe by electrophoresis on native 4% polyacrylamide gels and were then visualized by autoradiography of the dried gels. *E*, occupancy of the *GRHL2* promoter by ZEB1 *in vivo* as demonstrated by a ChIP assay. Cross-linked protein-chromatin complexes were enriched from MDA-MB-231 cells with two ZEB1-specific antibodies, clone H-102 (*lane 6*) and clone HPA027524 (*lane 7*). Omitting sera (*lane 3*) or using negative control IgG (*lane 4*) and positive control anti-RNA polymerase II antibody (*lane 5*) served as controls in these experiments, respectively. Input chromatin for each experiment is shown in *lane 2*. The immunoprecipitated chromatin was subjected to PCR amplification using primers flanking the ZEB1-binding site in the *GRHL2* regulatory region (*top*) or primers specific for the *GAPDH* promoter, which were used as a negative control (*bottom*). In control PCRs, input chromatin was omitted (*lane 1*). *Error bars*, S.D.

and histological tumor type, we also stained a breast cancer prognosis tissue microarray containing about 2000 tissue samples. The results summarized in supplemental Table 2 show that GRHL2 expression is significantly associated with estrogen and progesterone receptor expression ($p < 0.0001$). Also, we found statistically significant inverse correlations between an increased intensity of GRHL2 expression and increased tumor stages ($p < 0.0001$) or the presence of lymph node metastases ($p = 0.023$). Thus, the results

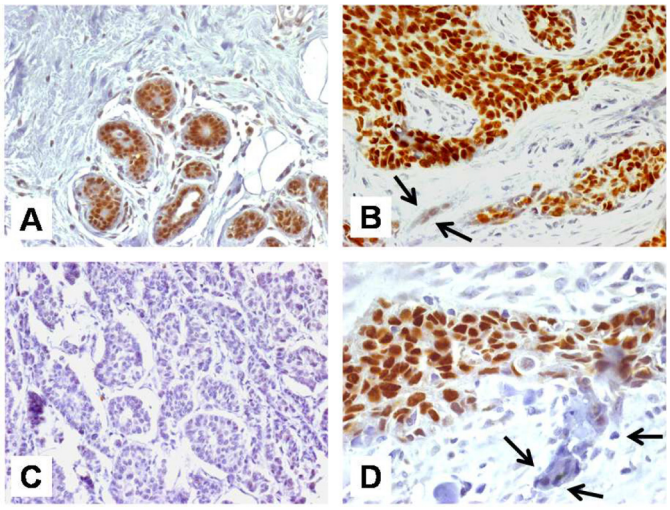


FIGURE 8. **Immunohistochemical analysis of GRHL2 expression in primary breast cancers.** An immunohistochemical staining of formalin-fixed, paraffin-embedded breast carcinoma tissues using a GRHL2-specific polyclonal antibody was performed. Representative images illustrative of the different staining patterns are presented. *A*, nuclear staining of GRHL2 in normal breast epithelium adjacent to invasive ductal carcinoma shown in *B*. *B*, invasive ductal carcinoma showing strong nuclear staining for GRHL2. *C*, invasive ductal carcinoma showing no staining for GRHL2. *D*, invasive ductal carcinoma as in *B* at higher magnification. Loss of *GRHL2* expression in tumor cells that bud off from the main tumor mass and in individual tumor cells with no discernible continuity with the parent tumor is indicated with *arrows* in *B* and *D*. Original magnification, ×200 (*A*–*C*) and ×400 (*D*).

of our immunohistochemical study again point to a role of *GRHL2* during EMT in breast carcinogenesis.

## DISCUSSION

The identification and structural and functional characterization of novel cancer-related genes are a prerequisite for a better understanding of the molecular mechanisms driving carcinogenesis and for the development of innovative therapeutic approaches for the treatment of cancer patients. To isolate novel protooncogenes, a retrovirus-mediated cDNA expression cloning approach utilizing preneoplastic, murine NIH3T3 fibroblasts was employed. Using this genetic screen, we identified the GRHL2 transcription factor as a novel protooncogene capable of transforming NIH3T3 fibroblasts. GRHL2 therefore represents the first member of the grainyhead family of transcription factors known to induce malignant transformation of cells. We also describe the existence of GRHL2 isoforms generated by alternative splicing of the primary *GRHL2* gene transcript and provide evidence that the corresponding gene products exhibit dominant negative effects on canonical GRHL2 proteins. These findings potentially could represent a novel mechanism of regulating GRHL2 activity in cancer cells.

To molecularly define the tumor-promoting activities of *GRHL2*, it was pivotal to identify potential GRHL2 target genes. A dual strategy combining gene expression analysis and a phylogenetic footprinting analysis was pursued and resulted in the identification of a large number of genes predicted to be directly regulated by GRHL2 ($n = 73$), including the accepted GRHL2 target genes *Arhgef19* (7) and *Fas* (17) and, most importantly, also the EGFR family member *ERBB3*. The identification of *ERBB3* as a GRHL2 target gene in breast cancer cells has very important implications for breast cancer in that aberrant activation of ERBB3, which forms oncogenic heterodimers with ERBB2 (HER2), has been linked to decreased survival in breast cancer (42) and has been functionally involved in resistance to targeted therapies, such as tamoxifen (43, 44), trastuzumab (45, 46), lapatinib (47), and gefitinib (48, 49).

Our findings, however, are based on studies performed using murine NIH3T3 fibroblasts as a model system. A key question, therefore, is the pathophysiological relevance of our observations for human breast carcinogenesis. To address this issue, we stably overexpressed GRHL2 transcription factor in GRHL2-deficient human breast cancer cell lines and analyzed its influence on cell proliferation. Consistent with results recently published by Cieply *et al.* (19), no significant impact on the rate of cell proliferation of any basal-B type of breast cancer cell line (*e.g.* MDA-MB-231 and BT-549 cells) could be observed. By contrast, shRNA-mediated knockdown of *GRHL2* expression or functional inactivation of *GRHL2* using GRHL2-DN proteins in a variety of *GRHL2*-expressing breast cancer cell lines resulted in a dramatic reduction of cell proliferation, suggesting that *GRHL2* indeed exhibits strong tumor-promoting activities in a breast cancer subtype-specific fashion. The activity of a transcription factor in a cell depends on a variety of factors, including its expression level, the state of activity (which often is determined by various post-translational modifications), the presence of essential co-factors, and the occupancy of the regulatory region of target genes by other transcriptional regulators, to name a few. It is likely that essential co-factors are missing in the poorly differentiated, basal-B type human breast cancer cell lines to support *GRHL2*-driven regulation of epithelial cell proliferation.

Importantly, loss of *GRHL2* expression in breast cancer cells is associated with EMT-like morphological changes and increased cell survival and migratory and invasive behavior of cells. Accordingly, reexpression of *GRHL2* in *GRHL2*-deficient basal-B type breast cancer cell lines caused phenotypical alterations indicative of the inverse process, the MET. Thus, our data in conjunction with results recently published by others (19, 20) certainly allow GRHL2 to be classified as an EMT suppressor molecule. The analysis of *GRHL2*-induced gene expression changes in our experimental model systems showing significant changes of selected EMT marker genes (*e.g. CDH1*, *DSC2*, *ZO-1*, *KRT* genes, *CLDN* genes, *VIM*, *ZEB1*, and *CD24* stem cell marker) further support an important role of *GRHL2* in regulating EMT. Overall, the *GRHL2*-dependent phenotypical and gene expression changes in our experimental systems were more pronounced in *GRHL2*-overexpressing cells than in *GRHL2* knockdown experiments. Presumably, lentivirally delivered shRNAs may not lower the level of *GRHL2* expression below that needed for full binding site occupancy of target genes; therefore, expression of GRHL2 target genes will be less affected. The experimental limitations of the siRNA technology in transcription factor biology are widely recognized (50).

The concept of coupling EMT with reduced cell proliferation is not novel, and other molecules controlling both processes, such as the YB-1 factor, could be identified (51, 52). Although hyperproliferation generally is considered to be a hallmark of cancer cells, it has been hypothesized that hyperproliferation may in fact be detrimental to survival during tumor cell dissem-

ination and metastasis (52). Shutdown of cell proliferation to preserve genomic integrity and to reduce the metabolic demands of cellular proliferation and, additionally, an increasing capability of anchorage-independent growth is beneficial for survival of carcinoma cells in the circulation and in the hostile microenvironment of secondary organs. A low proliferative activity may represent an integral part of the mesenchymal phenotype, allowing cancer cells to migrate and disseminate to secondary organs before reinitiating tumor cell growth (51). A frequent clinical observation in breast cancer is that recurrence of overt metastasis may occur many years after the removal of or seemingly successful therapy for the primary tumor. Presumably malignant cells, shed from the primary tumor mass, remain dormant but still viable all the time, only to express their tumorigenic potential at a later time point. The presence of micrometastatic, dormant cells is an accepted indicator of recurrent disease and poor prognosis (53, 54). However, the molecular mechanisms allowing carcinoma cells to escape from dormancy still remain enigmatic. It is entirely conceivable that genes regulating EMT/MET processes as well as tumor cell proliferation and cancer cell survival, such as the EMT suppressor molecule GRHL2, represent prime candidate genes crucial for the establishment of clinically detectable metastases.

Another very important finding of our study is that expression of *GRHL2* is repressed by the ZEB1 transcription factor in breast cancer cells. On the other hand, we also provide evidence that repression of GRHL2 function leads to an up-regulation of *ZEB1* expression in breast cancer cells. In fact, the *ZEB1* transcription factor very recently has convincingly been shown to be a direct target for repression by GRHL2 (19), suggesting that GRHL2 and ZEB1 transcription factors form a double negative regulatory feedback loop. It is important to note that ZEB1 also transcriptionally represses genes of the *miR-200* family, which in turn post-transcriptionally inhibit expression of *ZEB1* by binding to a highly conserved target site within the 3′-untranslated region (55) and that GRHL2 has been reported to up-regulate the expression of *miR-200b/c* family members in breast cancer cells (19). Collectively, our data therefore suggest the existence of a highly complex, interconnected GRHL2/ZEB1/miR-200 regulatory system. Interestingly, a feedback loop consisting of GRHL2 and Nkx2–1 transcription factors has also been demonstrated to exist in lung epithelium (56), implying that feedback loop regulation of *GRHL2* expression may emerge as a common theme in epithelial cell morphogenesis and differentiation. Autoregulatory transcriptional feedback loops result in a fine tuning of gene expression, stabilize transcriptional activity to withstand changes in microenvironmental cues, or reinforce changes in gene expression upon stimulation of cells by extracellular stimuli. Therefore, disruption of the GRHL2/ZEB1/miR-200 transcriptional regulatory network controlling EMT may ultimately contribute to breast cancer metastasis.

Conflicting results regarding *GRHL2* expression in primary breast cancers and also its activity in breast cancer model systems were reported very recently (19, 20, 57). The results of our study, which represents the first comprehensive immunohistochemical analysis of GRHL2 protein expression in a certain tumor, point to an important role of *GRHL2* during EMT in breast carcinogenesis. Although based on relatively small numbers, we found a statistically significant association between loss of *GRHL2* expression and the presence of lymph node metastases in breast cancer ($p = 0.023$). Furthermore, we also observed a striking loss of *GRHL2* expression in tumor cells that bud off from the main tumor mass and in individual tumor cells with no discernible continuity with the parent tumor. Cells that have undergone EMT typically constitute a minor proportion of the primary tumor and are primarily found at tumor margins and have a low proliferative potential. In light of this, the results of our immunohistochemical analysis further substantiate an important role of *GRHL2* during EMT in breast cancer. On the other hand, evidence was also reported for an up-regulation of *GRHL2* expression in the majority of breast cancers except for those belonging to the "claudin-low" subclass as compared with normal breast tissues (19, 20, 57). Consistent with its fundamental role in preserving epithelial cell integrity, we observed strong *GRHL2* expression in normal breast epithelium, which appeared not to be substantially lower than in tumor tissues. As discussed by Cieply *et al.* (19), an apparent up-regulation of *GRHL2* mRNA, as determined by analysis of gene expression data sets, could represent an artifactual result of expansion of the epithelial cell compartment relative to normal mammary gland during tumor outgrowth. Still, an elevated *GRHL2* expression also has been reported to correlate with a shorter relapse-free survival interval and increased risk of metastasis in breast cancer patients (20). These findings are supported by functional studies showing that overexpression of *Grhl2* in murine 4T1 breast cancer cells significantly promotes tumor growth and metastasis (20). The discrepancies in results became even more apparent when *GRHL2* expression and activity was analyzed in the non-tumorigenic epithelial cell line MCF-10A. Consistent with data published by Cieply *et al.* (19), we observed only very low levels of *GRHL2* expression in this experimental system. Xiang *et al.* (20) reported significant *GRHL2* expression in these cells, as determined by non-quantitative RT-PCR analysis, and demonstrated that knockdown of *GRHL2* in MCF-10A cells induced EMT-like changes. Conversely, Yang *et al.* (57) very recently showed that overexpression of *Grhl2* in MCF-10A cells provoked a mesenchymal phenotype, whereas we provide evidence herein that overexpression of *GRHL2* rather preserves epithelial cell integrity and antagonizes TGF-$\beta$-induced EMT in MCF-10A cells. At present, the reasons for obvious discrepancies in results from different studies are completely unclear. Further studies are therefore needed to unravel the still enigmatic and even contradictory roles of the EMT suppressor molecule GRHL2 in breast carcinogenesis.

*Acknowledgments—We thank Sonja Santjer and Malgorzata Stoupiec for excellent technical assistance.*

## REFERENCES

1. Wilanowski, T., Tuckfield, A., Cerruti, L., O'Connell, S., Saint, R., Parekh, V., Tao, J., Cunningham, J. M., and Jane, S. M. (2002) A highly conserved novel family of mammalian developmental transcription factors related to *Drosophila* grainyhead. *Mech. Dev.* **114,** 37–50
2. Kudryavtseva, E. I., Sugihara, T. M., Wang, N., Lasso, R. J., Gudnason, J. F., Lipkin, S. M., and Andersen, B. (2003) Identification and characterization

of Grainyhead-like epithelial transactivator (GET-1), a novel mammalian Grainyhead-like factor. *Dev. Dyn.* **226,** 604–617
3. Ting, S. B., Wilanowski, T., Cerruti, L., Zhao, L. L., Cunningham, J. M., and Jane, S. M. (2003) The identification and characterization of human Sister-of-Mammalian Grainyhead (SOM) expands the grainyhead-like family of developmental transcription factors. *Biochem. J.* **370,** 953–962
4. Auden, A., Caddy, J., Wilanowski, T., Ting, S. B., Cunningham, J. M., and Jane, S. M. (2006) Spatial and temporal expression of the Grainyhead-like transcription factor family during murine development. *Gene Expr. Patterns* **6,** 964–970
5. Werth, M., Walentin, K., Aue, A., Schönheit, J., Wuebken, A., Pode-Shakked, N., Vilianovitch, L., Erdmann, B., Dekel, B., Bader, M., Barasch, J., Rosenbauer, F., Luft, F. C., and Schmidt-Ott, K. M. (2010) The transcription factor grainyhead-like 2 regulates the molecular composition of the epithelial apical junctional complex. *Development* **137,** 3835–3845
6. Pyrgaki, C., Liu, A., and Niswander, L. (2011) Grainyhead-like 2 regulates neural tube closure and adhesion molecule expression during neural fold fusion. *Dev. Biol.* **353,** 38–49
7. Boglev, Y., Wilanowski, T., Caddy, J., Parekh, V., Auden, A., Darido, C., Hislop, N. R., Cangkrama, M., Ting, S. B., and Jane, S. M. (2011) The unique and cooperative roles of the Grainy head-like transcription factors in epidermal development reflect unexpected target gene specificity. *Dev. Biol.* **349,** 512–522
8. Dworkin, S., Darido, C., Georgy, S. R., Wilanowski, T., Srivastava, S., Ellett, F., Pase, L., Han, Y., Meng, A., Heath, J. K., Lieschke, G. J., and Jane, S. M. (2012) Midbrain-hindbrain boundary patterning and morphogenesis are regulated by diverse grainy head-like 2-dependent pathways. *Development* **139,** 525–536
9. Rifat, Y., Parekh, V., Wilanowski, T., Hislop, N. R., Auden, A., Ting, S. B., Cunningham, J. M., and Jane, S. M. (2010) Regional neural tube closure defined by the Grainy head-like transcription factors. *Dev. Biol.* **345,** 237–245
10. Mace, K. A., Pearson, J. C., and McGinnis, W. (2005) An epidermal barrier wound repair pathway in *Drosophila* is mediated by grainy head. *Science* **308,** 381–385
11. Ting, S. B., Caddy, J., Hislop, N., Wilanowski, T., Auden, A., Zhao, L. L., Ellis, S., Kaur, P., Uchida, Y., Holleran, W. M., Elias, P. M., Cunningham, J. M., and Jane, S. M. (2005) A homolog of *Drosophila* grainy head is essential for epidermal integrity in mice. *Science* **308,** 411–413
12. Moussian, B., and Uv, A. E. (2005) An ancient control of epithelial barrier formation and wound healing. *BioEssays* **27,** 987–990
13. Bissell, M. J., and Radisky, D. (2001) Putting tumours in context. *Nat. Rev. Cancer* **1,** 46–54
14. Dvorak, H. F. (1986) Tumors. Wounds that do not heal. Similarities between tumor stroma generation and wound healing. *N. Engl. J. Med.* **315,** 1650–1659
15. Chen, W., Dong, Q., Shin, K. H., Kim, R. H., Oh, J. E., Park, N. H., and Kang, M. K. (2010) Grainyhead-like 2 enhances the hTERT gene expression by inhibiting DNA methylation at the 5′-CpG island in normal human keratinocytes. *J. Biol. Chem.* **285,** 40852–40863
16. Kang, X., Chen, W., Kim, R. H., Kang, M. K., and Park, N. H. (2009) Regulation of the hTERT promoter activity by MSH2, the hnRNPs K and D, and GRHL2 in human oral squamous cell carcinoma cells. *Oncogene* **28,** 565–574
17. Dompe, N., Rivers, C. S., Li, L., Cordes, S., Schwickart, M., Punnoose, E. A., Amler, L., Seshagiri, S., Tang, J., Modrusan, Z., and Davis, D. P. (2011) A whole-genome RNAi screen identifies an 8q22 gene cluster that inhibits death receptor-mediated apoptosis. *Proc. Natl. Acad. Sci. U.S.A.* **108,** E943–E951
18. Tanaka, Y., Kanai, F., Tada, M., Tateishi, R., Sanada, M., Nannya, Y., Ohta, M., Asaoka, Y., Seto, M., Shiina, S., Yoshida, H., Kawabe, T., Yokosuka, O., Ogawa, S., and Omata, M. (2008) Gain of GRHL2 is associated with early recurrence of hepatocellular carcinoma. *J. Hepatol.* **49,** 746–757
19. Cieply, B., Riley, P., 4th, Pifer, P. M., Widmeyer, J., Addison, J. B., Ivanov, A. V., Denvir, J., and Frisch, S. M. (2012) Suppression of the epithelial-mesenchymal transition by Grainyhead-like-2. *Cancer Res.* **72,** 2440–2453
20. Xiang, X., Deng, Z., Zhuang, X., Ju, S., Mu, J., Jiang, H., Zhang, L., Yan, J., Miller, D., and Zhang, H. G. (2012) Grhl2 determines the epithelial phenotype of breast cancers and promotes tumor progression. *PLoS One* **7,** e50781
21. Assmann, V., Marshall, J. F., Fieber, C., Hofmann, M., and Hart, I. R. (1998) The human hyaluronan receptor RHAMM is expressed as an intracellular protein in breast cancer cells. *J. Cell Sci.* **111,** 1685–1694
22. Hobbs, S., Jitrapakdee, S., and Wallace, J. C. (1998) Development of a bicistronic vector driven by the human polypeptide chain elongation factor 1$\alpha$ promoter for creation of stable mammalian cell lines that express very high levels of recombinant proteins. *Biochem. Biophys. Res. Commun.* **252,** 368–372
23. Stanton, V. P., Jr., Nichols, D. W., Laudano, A. P., and Cooper, G. M. (1989) Definition of the human raf amino-terminal regulatory region by deletion mutagenesis. *Mol. Cell Biol.* **9,** 639–647
24. Ausubel, F. M., Brent, R., Kingston, R. E., Moore, D. D., Seidman, J. G., Smith, J. A., and Struhl, K. (eds) (2001) *Current Protocols in Molecular Biology*, John Wiley & Sons, Inc., New York
25. Altschul, S. F., Gish, W., Miller, W., Myers, E. W., and Lipman, D. J. (1990) Basic local alignment search tool. *J. Mol. Biol.* **215,** 403–410
26. Cox, A. D., and Der, C. J. (1994) Biological assays for cellular transformation. *Methods Enzymol.* **238,** 277–294
27. Gentleman, R. C., Carey, V. J., Bates, D. M., Bolstad, B., Dettling, M., Dudoit, S., Ellis, B., Gautier, L., Ge, Y., Gentry, J., Hornik, K., Hothorn, T., Huber, W., Iacus, S., Irizarry, R., Leisch, F., Li, C., Maechler, M., Rossini, A. J., Sawitzki, G., Smith, C., Smyth, G., Tierney, L., Yang, J. Y., and Zhang, J. (2004) Bioconductor. Open software development for computational biology and bioinformatics. *Genome Biol.* **5,** R80
28. Assmann, V., Jenkinson, D., Marshall, J. F., and Hart, I. R. (1999) The intracellular hyaluronan receptor RHAMM/IHABP interacts with microtubules and actin filaments. *J. Cell Sci.* **112,** 3943–3954
29. Kristiansen, G., Machado, E., Bretz, N., Rupp, C., Winzer, K. J., König, A. K., Moldenhauer, G., Marmé, F., Costa, J., and Altevogt, P. (2010) Molecular and clinical dissection of CD24 antibody specificity by a comprehensive comparative analysis. *Lab. Invest.* **90,** 1102–1116
30. Moffat, J., Grueneberg, D. A., Yang, X., Kim, S. Y., Kloepfer, A. M., Hinkle, G., Piqani, B., Eisenhaure, T. M., Luo, B., Grenier, J. K., Carpenter, A. E., Foo, S. Y., Stewart, S. A., Stockwell, B. R., Hacohen, N., Hahn, W. C., Lander, E. S., Sabatini, D. M., and Root, D. E. (2006) A lentiviral RNAi library for human and mouse genes applied to an arrayed viral high-content screen. *Cell* **124,** 1283–1298
31. Andrews, N. C., and Faller, D. V. (1991) A rapid micropreparation technique for extraction of DNA-binding proteins from limiting numbers of mammalian cells. *Nucleic Acids Res.* **19,** 2499
32. Flicek, P., Amode, M. R., Barrell, D., Beal, K., Brent, S., Chen, Y., Clapham, P., Coates, G., Fairley, S., Fitzgerald, S., Gordon, L., Hendrix, M., Hourlier, T., Johnson, N., Kähäri, A., Keefe, D., Keenan, S., Kinsella, R., Kokocinski, F., Kulesha, E., Larsson, P., Longden, I., McLaren, W., Overduin, B., Pritchard, B., Riat, H. S., Rios, D., Ritchie, G. R., Ruffier, M., Schuster, M., Sobral, D., Spudich, G., Tang, Y. A., Trevanion, S., Vandrovcova, J., Vilella, A. J., White, S., Wilder, S. P., Zadissa, A., Zamora, J., Aken, B. L., Birney, E., Cunningham, F., Dunham, I., Durbin, R., Fernández-Suarez, X. M., Herrero, J., Hubbard, T. J., Parker, A., Proctor, G., Vogel, J., and Searle, S. M. (2011) Ensembl 2011. *Nucleic Acids Res.* **39,** D800–D806
33. Thomas-Chollier, M., Defrance, M., Medina-Rivera, A., Sand, O., Herrmann, C., Thieffry, D., and van Helden, J. (2011) RSAT 2011. regulatory sequence analysis tools. *Nucleic Acids Res.* **39,** W86–W91
34. ENCODE Project Consortium (2011) A user's guide to the encyclopedia of DNA elements (ENCODE). *PLoS Biol.* **9,** e1001046
35. Spaderna, S., Schmalhofer, O., Hlubek, F., Berx, G., Eger, A., Merkel, S., Jung, A., Kirchner, T., and Brabletz, T. (2006) A transient, EMT-linked loss of basement membranes indicates metastasis and poor survival in colorectal cancer. *Gastroenterology* **131,** 830–840
36. Edgar, R. C. (2004) MUSCLE. Multiple sequence alignment with high accuracy and high throughput. *Nucleic Acids Res.* **32,** 1792–1797
37. Okonechnikov, K., Golosova, O., and Fursov, M. (2012) Unipro UGENE. A unified bioinformatics toolkit. *Bioinformatics* **28,** 1166–1167
38. Simon, R., and Sauter, G. (2002) Tissue microarrays for miniaturized high-throughput molecular profiling of tumors. *Exp. Hematol.* **30,** 1365–1372

39. Kozak, M. (1989) The scanning model for translation. An update. *J. Cell Biol.* **108,** 229–241
40. Neve, R. M., Chin, K., Fridlyand, J., Yeh, J., Baehner, F. L., Fevr, T., Clark, L., Bayani, N., Coppe, J. P., Tong, F., Speed, T., Spellman, P. T., DeVries, S., Lapuk, A., Wang, N. J., Kuo, W. L., Stilwell, J. L., Pinkel, D., Albertson, D. G., Waldman, F. M., McCormick, F., Dickson, R. B., Johnson, M. D., Lippman, M., Ethier, S., Gazdar, A., and Gray, J. W. (2006) A collection of breast cancer cell lines for the study of functionally distinct cancer subtypes. *Cancer Cell* **10,** 515–527
41. Brown, K. A., Aakre, M. E., Gorska, A. E., Price, J. O., Eltom, S. E., Pietenpol, J. A., and Moses, H. L. (2004) Induction by transforming growth factor-$\beta$1 of epithelial to mesenchymal transition is a rare event *in vitro*. *Breast Cancer Res.* **6,** R215–R231
42. Sithanandam, G., and Anderson, L. M. (2008) The ERBB3 receptor in cancer and cancer gene therapy. *Cancer Gene Ther.* **15,** 413–448
43. Folgiero, V., Avetrani, P., Bon, G., Di Carlo, S. E., Fabi, A., Nisticò, C., Vici, P., Melucci, E., Buglioni, S., Perracchio, L., Sperduti, I., Rosanò, L., Sacchi, A., Mottolese, M., and Falcioni, R. (2008) Induction of ErbB-3 expression by $\alpha$6$\beta$4 integrin contributes to tamoxifen resistance in ER$\beta$1-negative breast carcinomas. *PLoS One* **3,** e1592
44. Liu, B., Ordonez-Ercan, D., Fan, Z., Edgerton, S. M., Yang, X., and Thor, A. D. (2007) Downregulation of erbB3 abrogates erbB2-mediated tamoxifen resistance in breast cancer cells. *Int. J. Cancer* **120,** 1874–1882
45. Wang, S. E., Xiang, B., Guix, M., Olivares, M. G., Parker, J., Chung, C. H., Pandiella, A., and Arteaga, C. L. (2008) Transforming growth factor $\beta$ engages TACE and ErbB3 to activate phosphatidylinositol-3 kinase/Akt in ErbB2-overexpressing breast cancer and desensitizes cells to trastuzumab. *Mol. Cell Biol.* **28,** 5605–5620
46. Narayan, M., Wilken, J. A., Harris, L. N., Baron, A. T., Kimbler, K. D., and Maihle, N. J. (2009) Trastuzumab-induced HER reprogramming in "resistant" breast carcinoma cells. *Cancer Res.* **69,** 2191–2194
47. Garrett, J. T., Olivares, M. G., Rinehart, C., Granja-Ingram, N. D., Sánchez, V., Chakrabarty, A., Dave, B., Cook, R. S., Pao, W., McKinely, E., Manning, H. C., Chang, J., and Arteaga, C. L. (2011) Transcriptional and posttranslational up-regulation of HER3 (ErbB3) compensates for inhibition of the HER2 tyrosine kinase. *Proc. Natl. Acad. Sci. U.S.A.* **108,** 5021–5026
48. Engelman, J. A., Zejnullahu, K., Mitsudomi, T., Song, Y., Hyland, C., Park, J. O., Lindeman, N., Gale, C. M., Zhao, X., Christensen, J., Kosaka, T., Holmes, A. J., Rogers, A. M., Cappuzzo, F., Mok, T., Lee, C., Johnson, B. E., Cantley, L. C., and Jänne, P. A. (2007) MET amplification leads to gefitinib resistance in lung cancer by activating ERBB3 signaling. *Science* **316,** 1039–1043
49. Sergina, N. V., Rausch, M., Wang, D., Blair, J., Hann, B., Shokat, K. M., and Moasser, M. M. (2007) Escape from HER-family tyrosine kinase inhibitor therapy by the kinase-inactive HER3. *Nature* **445,** 437–441
50. Farnham, P. J. (2009) Insights from genomic profiling of transcription factors. *Nat. Rev. Genet.* **10,** 605–616
51. Evdokimova, V., Tognon, C., Ng, T., Ruzanov, P., Melnyk, N., Fink, D., Sorokin, A., Ovchinnikov, L. P., Davicioni, E., Triche, T. J., and Sorensen, P. H. (2009) Translational activation of snail1 and other developmentally regulated transcription factors by YB-1 promotes an epithelial-mesenchymal transition. *Cancer Cell* **15,** 402–415
52. Evdokimova, V., Tognon, C., Ng, T., and Sorensen, P. H. (2009) Reduced proliferation and enhanced migration. Two sides of the same coin? Molecular mechanisms of metastatic progression by YB-1. *Cell Cycle* **8,** 2901–2906
53. Braun, S., Pantel, K., Müller, P., Janni, W., Hepp, F., Kentenich, C. R., Gastroph, S., Wischnik, A., Dimpfl, T., Kindermann, G., Riethmüller, G., and Schlimok, G. (2000) Cytokeratin-positive cells in the bone marrow and survival of patients with stage I, II, or III breast cancer. *N. Engl. J. Med.* **342,** 525–533
54. Braun, S., Vogl, F. D., Naume, B., Janni, W., Osborne, M. P., Coombes, R. C., Schlimok, G., Diel, I. J., Gerber, B., Gebauer, G., Pierga, J. Y., Marth, C., Oruzio, D., Wiedswang, G., Solomayer, E. F., Kundt, G., Strobl, B., Fehm, T., Wong, G. Y., Bliss, J., Vincent-Salomon, A., and Pantel, K. (2005) A pooled analysis of bone marrow micrometastasis in breast cancer. *N. Engl. J. Med.* **353,** 793–802
55. Brabletz, S., and Brabletz, T. (2010) The ZEB/miR-200 feedback loop. A motor of cellular plasticity in development and cancer? *EMBO Rep.* **11,** 670–677
56. Varma, S., Cao, Y., Tagne, J. B., Lakshminarayanan, M., Li, J., Friedman, T. B., Morell, R. J., Warburton, D., Kotton, D. N., and Ramirez, M. I. (2012) The transcription factors grainyhead-like 2 and NK2 homeobox 1 form a regulatory loop that coordinates lung epithelial cell morphogenesis and differentiation. *J. Biol. Chem.* **287,** 37282–37295
57. Yang, X., Vasudevan, P., Parekh, V., Penev, A., and Cunningham, J. M. (2013) Bridging cancer biology with the clinic. Relative expression of a GRHL2-mediated gene-set pair predicts breast cancer metastasis. *PLoS One* **8,** e56195